Semileptonic and Leptonic Rare B Decays (Lecture # 4)

Ahmed Ali

DESY (Hamburg) & KEK, Tsukuba

Contents

- Effective Hamiltonian in SM
- The Decay $B \to X_s \ell^+ \ell^-$ in the SM & Experiments
- Exclusive Decays $B \to (K, K^*) \ell^+ \ell^-$ in the SM and Current Data
- CKM-Suppressed Semileptonic Decays $B \to X_d \ell^+ \ell^-$ and $B_s \to X_s \ell^+ \ell^-$ in the SM and Prospects of Measurements at LHC-B and Super-B-Factory
- $B \to X_s(X_d) \nu \bar{\nu}$ Decays in the SM
- $B_s(B_d) \to \ell^+ \ell^-$ Decays in the SM
- Summary on Rare B-Decays

Lecture Series: KEK, December 4 - 22, 2003

hep-ph/0312303

KEK-TH-928
hep-ph/0312303

CKM Phenomenology and B-Meson Physics - Present Status and Current Issues

Ahmed Ali

Theory Group, High Energy Accelerator Research Organization (KEK), Tsukuba, 305 -0801, Japan [a]

December 22, 2003

Abstract

We review the status of the Cabibbo-Kobayashi-Maskawa (CKM) matrix elements and the CP-violating phases in the CKM-unitarity triangle. The emphasis in these lecture notes is on B-meson physics, though we also review the current status and issues in the light quark sector of this matrix. Selected applications of theoretical methods in QCD used in the interpretation of data are given and some of the issues restricting the theoretical precision on the CKM matrix elements discussed. The overall consistency of the CKM theory with the available data in flavour physics is impressive and we quantify this consistency. Current data also show some anomalies which, however, are not yet statistically significant. They are discussed briefly. Some benchmark measurements that remain to be done in experiments at the B-factories and hadron colliders are listed. Together with the already achieved results, they will provide unprecedented tests of the CKM theory and by the same token may lead to the discovery of new physics.

To appear in the Proceedings of the International Meeting on Fundamental Physics, Soto de Cangas (Asturias), Spain, February 23 - 28, 2003; Publishers: CIEMAT Editorial Service (Madrid, Spain); J. Cuevas and A. Ruiz. (Eds.)

[a] On leave of absence from Deutsches Elektronen-Synchrotron DESY, D-22603 Hamburg, FRG.
E-mail: ahmed@post.kek.jp

Effective Hamiltonian in SM

$$\mathcal{H}_{\text{eff}}(b \to s\gamma; b \to s\ell^+\ell^-) = -\frac{4G_F}{\sqrt{2}} V_{ts}^* V_{tb} \sum_{i=1}^{10} C_i(\mu)\, O_i(\mu)$$

- $O_i(\mu)$: Dimension-six operators at the scale μ
- $C_i(\mu)$: Corresponding Wilson coefficients
- G_F: Fermi coupling constant, V_{ij}: CKM matrix elements

Four-Quark Operators O_i $(i = 1, \ldots, 6)$

$$\begin{aligned}
O_1 &= (\bar{s}_L \gamma_\mu T^a c_L)(\bar{c}_L \gamma^\mu T^a b_L) \\
O_2 &= (\bar{s}_L \gamma_\mu c_L)(\bar{c}_L \gamma^\mu b_L) \\
O_3 &= (\bar{s}_L \gamma_\mu b_L) \textstyle\sum_q (\bar{q}\gamma^\mu q) \\
O_4 &= (\bar{s}_L \gamma_\mu T^a b_L) \textstyle\sum_q (\bar{q}\gamma^\mu T^a q) \\
O_5 &= (\bar{s}_L \gamma_{\mu_1}\gamma_{\mu_2}\gamma_{\mu_3} b_L) \textstyle\sum_q (\bar{q}\gamma^{\mu_1}\gamma^{\mu_2}\gamma^{\mu_3} q) \\
O_6 &= (\bar{s}_L \gamma_{\mu_1}\gamma_{\mu_2}\gamma_{\mu_3} T^a b_L) \textstyle\sum_q (\bar{q}\gamma^{\mu_1}\gamma^{\mu_2}\gamma^{\mu_3} T^a q)
\end{aligned}$$

Magnetic Moment Operators O_i $(i = 7, 8)$

$$O_7 = \frac{e}{g_s^2} m_b (\bar{s}_L \sigma^{\mu\nu} b_R) F_{\mu\nu}\,, \quad O_8 = \frac{1}{g_s} m_b (\bar{s}_L \sigma^{\mu\nu} T^a b_R) G^a_{\mu\nu}$$

Semileptonic FCNC Operators O_i $(i = 9, 10)$

$$O_9 = \frac{e^2}{g_s^2} (\bar{s}_L \gamma_\mu b_L) \textstyle\sum_\ell (\underbrace{\bar{\ell}\gamma^\mu \ell}_{\mathrm{V}})\,, \quad O_{10} = \frac{e^2}{g_s^2} (\bar{s}_L \gamma_\mu b_L) \textstyle\sum_\ell (\underbrace{\bar{\ell}\gamma^\mu \gamma_5 \ell}_{\mathrm{A}}$$

$B \to X_s \ell' \ell$

Effective Low Energy Hamiltonian

$$\mathcal{H}_{\rm eff}(b \to s\ell^+\ell^-) = -\frac{4G_F}{\sqrt{2}} V_{ts}^* V_{tb} \sum_{i=1}^{10} C_i(\mu) O_i(\mu)$$

- Obtained using the CKM unitarity & $V_{us}^* V_{ub} \ll V_{ts}^* V_{tb}$
- $O_{1,\ldots,6}$: 4-quark operators; O_8: bsg-Vertex; enter due to operator mixing and explicit $O(\alpha_s)$ corrections

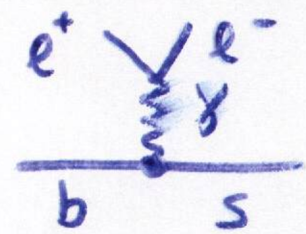

Dominant Operators

- $O_7 = \frac{e}{16\pi^2} \bar{s}_\alpha \sigma_{\mu\nu}(m_b R + m_s L) b_\alpha F^{\mu\nu}$
- $O_9 = \frac{e^2}{16\pi^2} \bar{s}_\alpha \gamma^\mu L b_\alpha \bar{\ell}\gamma_\mu \ell \quad (V)$
- $O_{10} = \frac{e^2}{16\pi^2} \bar{s}_\alpha \gamma^\mu L b_\alpha \bar{\ell}\gamma_\mu \gamma_5 \ell \quad (A)$

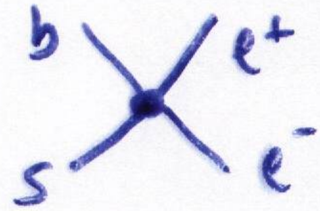

- Additional Non-local contribution to C_9

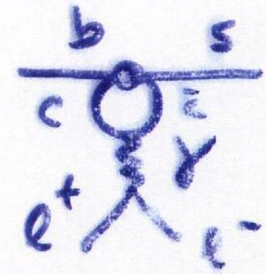

$$C_9^{\rm eff}(\hat{s}) = C_9 \eta(\hat{s}) + Y(\hat{s})$$

- $\eta(\hat{s}) = (1 + O(\alpha_s))$ [Jezabek, Kühn]
- $Y(\hat{s})$ contains perturbative charm loops and Charmonim resonances $(J/\psi, \psi', \ldots)$
- Several presciptions to combine SD- and Resonant parts [AA, Mannel, Morozumi '91; Krüger, Sehgal '96; ...]
- Residual uncertainty can be reduced by experimental cuts and using HQET $(1/m_c)$ power corrections
- FB Asymmetry $(z = \cos\theta_{\ell^+})$

$$\bar{A}_{FB}(s) = \frac{\int_{-1}^{1} \frac{d^2\Gamma}{ds\,dz}\,\mathrm{sgn}(z)\,dz}{\int_{-1}^{1} \frac{d^2\Gamma}{ds\,dz}\,dz}$$

$B \to X_s \ell' \ell$

Hiller, Handoko, Morozumi, A.
hep-ph/96094

Dilepton invariant mass distribution

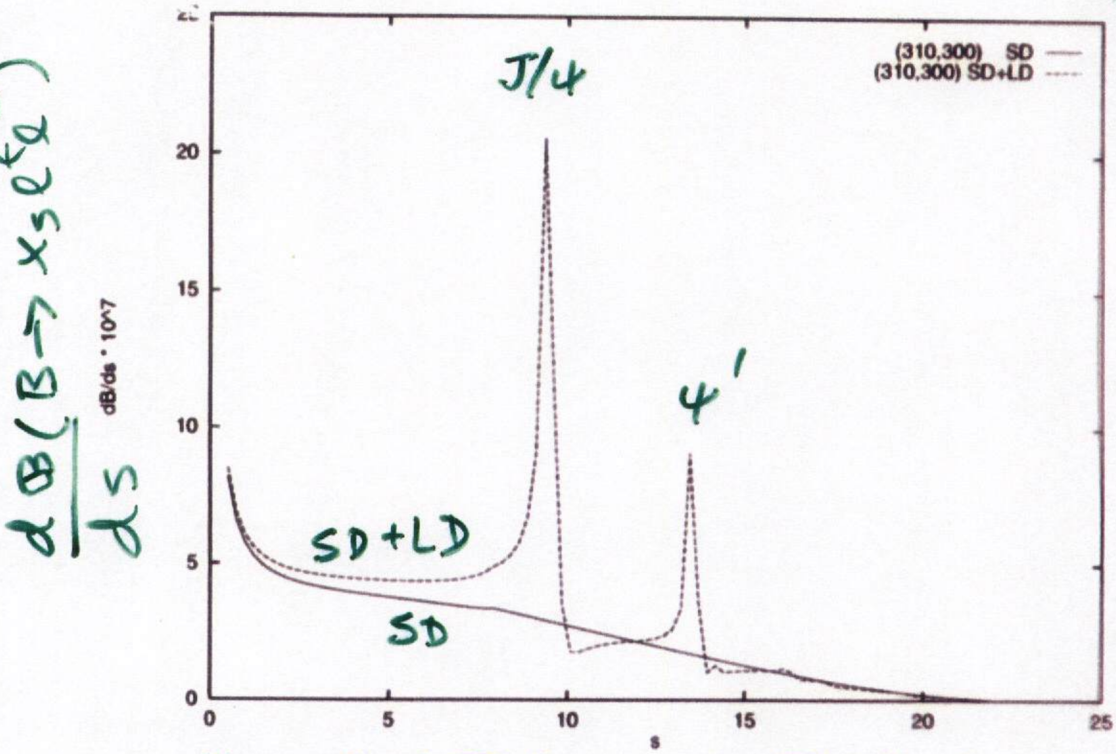

Normalized FB Asymmetry Distribution

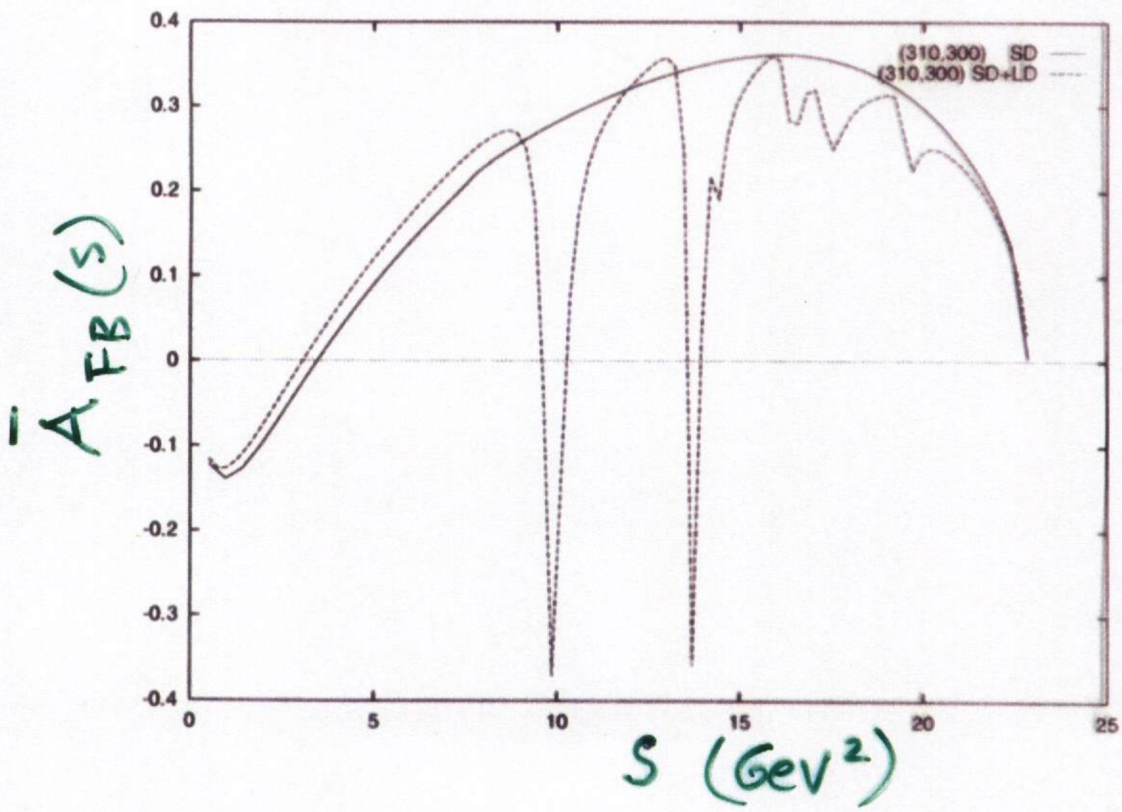

Inclusive $B \to X_s \ell^+ \ell^-$ in NNLO in SM

Dilepton Invariant Mass

$$\frac{d\Gamma(b \to X_s \ell^+ \ell^-)}{d\hat{s}} = \left(\frac{\alpha_{em}}{4\pi}\right)^2 \frac{G_F^2 m_{b,pole}^5 \left|V_{ts}^* V_{tb}\right|^2}{48\pi^3} (1-\hat{s})^2 \times$$

$$\left((1+2\hat{s})\left(\left|\tilde{C}_9^{\text{eff}}\right|^2 + \left|\tilde{C}_{10}^{\text{eff}}\right|^2\right) + 4\left(1+2/\hat{s}\right)\left|\tilde{C}_7^{\text{eff}}\right|^2 + 12\text{Re}\left(\tilde{C}_7^{\text{eff}} \tilde{C}_9^{\text{eff}*}\right)\right)$$

$$\begin{aligned}
\tilde{C}_7^{\text{eff}} &= \left(1 + \frac{\alpha_s(\mu)}{\pi}\omega_7(\hat{s})\right) A_7 \\
&\quad - \frac{\alpha_s(\mu)}{4\pi}\left(C_1^{(0)} F_1^{(7)}(\hat{s}) + C_2^{(0)} F_2^{(7)}(\hat{s}) + A_8^{(0)} F_8^{(7)}(\hat{s})\right), \\
\tilde{C}_9^{\text{eff}} &= \left(1 + \frac{\alpha_s(\mu)}{\pi}\omega_9(\hat{s})\right)\left(A_9 + T_9\, h(\hat{m}_c^2, \hat{s}) + U_9\, h(1, \hat{s}) + W_9\, h(0, \hat{s})\right) \\
&\quad - \frac{\alpha_s(\mu)}{4\pi}\left(C_1^{(0)} F_1^{(9)}(\hat{s}) + C_2^{(0)} F_2^{(9)}(\hat{s}) + A_8^{(0)} F_8^{(9)}(\hat{s})\right), \\
\tilde{C}_{10}^{\text{eff}} &= \left(1 + \frac{\alpha_s(\mu)}{\pi}\omega_9(\hat{s})\right) A_{10},
\end{aligned}$$

- $h(\hat{m}_c^2, \hat{s})$ **and** $\omega_9(\hat{s})$
  [Bobeth, Misiak; Urban NP B574 (2000) 291]
- $\omega_7(\hat{s})$, **and** $F_{1,2,8}^{(7,9)}(\hat{s})$
  [Asatrian, Asatrian, Greub, Walker; Phys. Lett. B507 (2001) 162; hep-ph/0109140]

- A_7, A_8, A_9, A_{10}, T_9, U_9, W_9 **are linear combinations of the Wilson coefficients**

NNLL Contributions in $B \to X_s \ell^+ \ell^-$

[Asatrian, Asatrian, Greub, Walker; Phys. Lett. B507 (2001) 162; hep-ph/0109140]

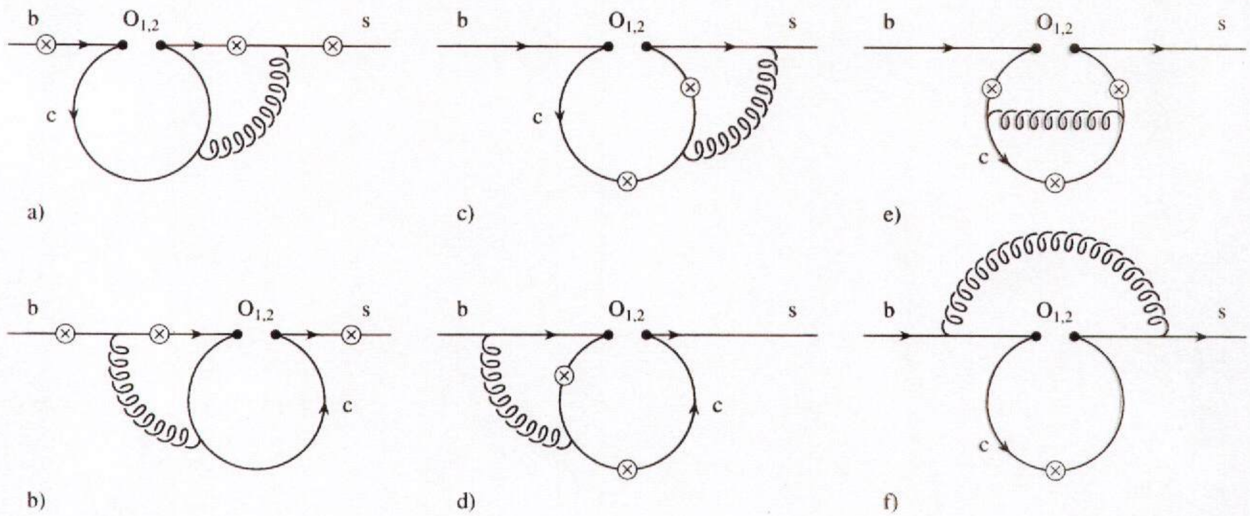

Figure 1: Matrix Elements from the operators $\mathcal{O}_{1,2}$

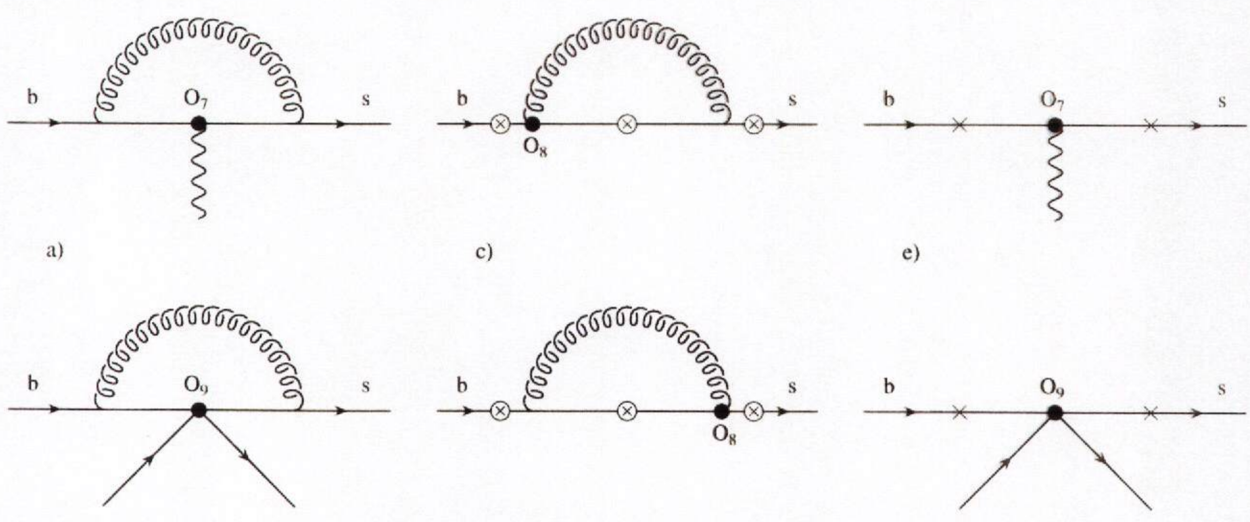

Figure 2: Matrix Elements from the operators $\mathcal{O}_7, \mathcal{O}_8, \mathcal{O}_9$

Power corrections in $B \to X_s \ell^+ \ell^-$ decays

- $1/m_b$ **corrections** [A. Falk et al., Phys. Rev. D49 (1994) 4553; AA, Handoko, Morozumi,Hiller, Phys. Rev. D55 (1997) 4105; Buchalla, Isidori, Rey; Nucl. Phys. B511 (1998) 594]

$$\frac{d\Gamma(b \to s\ell^+\ell^-)}{d\hat{s}} = \left(\frac{\alpha em}{4\pi}\right)^2 \frac{G_F^2 m_{b,pole}^5 |\lambda_{ts}|^2}{48\pi^3}(1-\hat{s})^2 \left[(1+2\hat{s})\left(\left|\widetilde{C}_9^{\text{eff}}\right|^2 + \left|\widetilde{C}_{10}^{\text{eff}}\right|^2\right) G\right.$$

$$+ \left. 4(1+2/\hat{s})\left|\widetilde{C}_7^{\text{eff}}\right|^2 G_2(\hat{s}) + 12\text{Re}\left(\widetilde{C}_7^{\text{eff}}\widetilde{C}_9^{\text{eff}*}\right) G_3(\hat{s}) + G_c(\hat{s})\right]$$

where

$$G_1(\hat{s}) = 1 + \frac{\lambda_1}{2m_b^2} + 3\frac{1-15\hat{s}^2+10\hat{s}^3}{(1-\hat{s})^2(1+2\hat{s})}\frac{\lambda_2}{2m_b^2}$$

$$G_2(\hat{s}) = 1 + \frac{\lambda_1}{2m_b^2} - 3\frac{6+3\hat{s}-5\hat{s}^3}{(1-\hat{s})^2(2+\hat{s})}\frac{\lambda_2}{2m_b^2}$$

$$G_3(\hat{s}) = 1 + \frac{\lambda_1}{2m_b^2} - \frac{5+6\hat{s}-7\hat{s}^2}{(1-\hat{s})^2}\frac{\lambda_2}{2m_b^2}$$

- $1/m_c$ **corrections** [Buchalla, Isidori, Rey; Nucl. Phys. B511 (1998) 594]

$$G_c(\hat{s}) = -\frac{8}{9}(C_2 - \frac{C_1}{6})\frac{\lambda_2}{m_c^2}\text{Re}\left(F(r)\left[\widetilde{C}_9^{\text{eff}*}(2+\hat{s}) + \widetilde{C}_7^{\text{eff}*}\frac{1+6\hat{s}-\hat{s}^2}{\hat{s}}\right]\right)$$

where $F(r)$ **(** $r = \hat{s}/(4\hat{m}_c^2)$**) is:**

$$F(r) = \frac{3}{2r}\begin{cases} \dfrac{1}{\sqrt{r(1-r)}}\arctan\sqrt{\dfrac{r}{1-r}} - 1 & 0 < r < 1 \\ \dfrac{1}{2\sqrt{r(r-1)}}\left(\ln\dfrac{1-\sqrt{1-1/r}}{1+\sqrt{1-1/r}} + i\pi\right) - 1 & r > 1 \end{cases}$$

(AA, Lunghi, Greub, Hiller

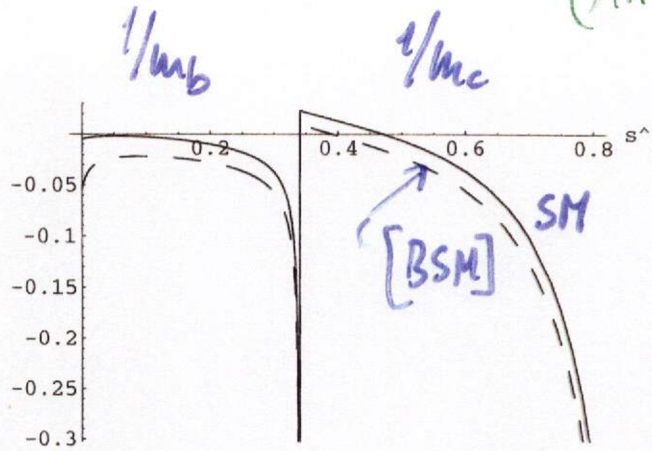

Power Corrections

Figure 4: Power correction $R(\hat{s})$ in decay rate for $B \to X_s \ell^+ \ell^-$: SM (solid), $C_7 = -C_7^{SM}$ (dashed)

Scale-dependence

$B \to X_s e^+ e^-$ $\quad$ $B \to X_s \ell^+ \ell^-$ $\ell = e, \mu$

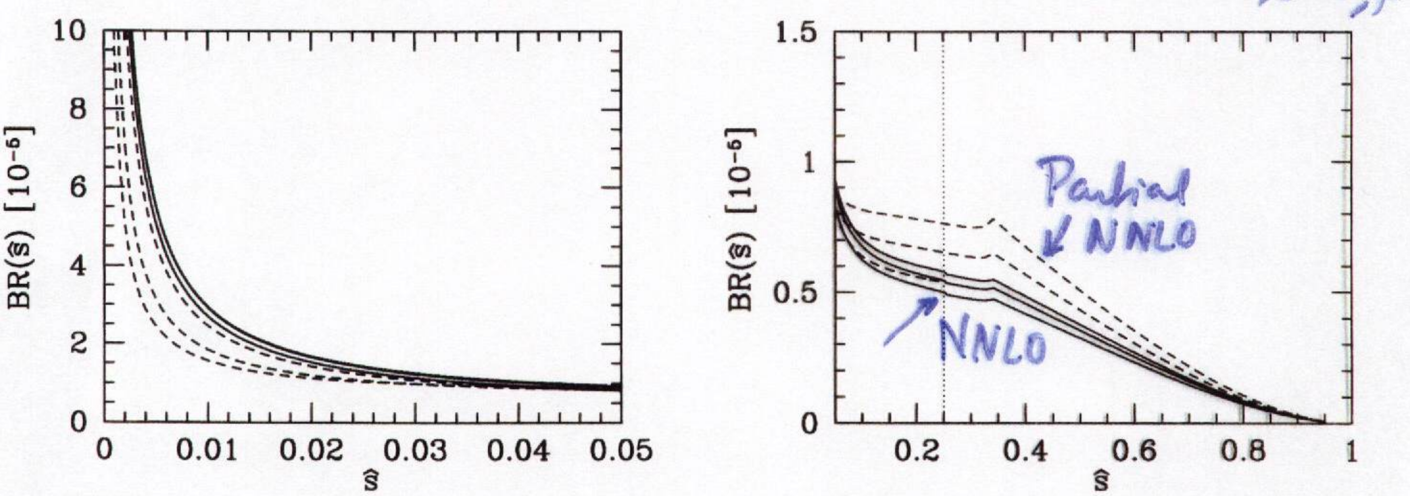

Figure 5: Dilepton inv. mass distributions in $B \to X_s \ell^+ \ell^-$; Partial NNLO (dashed lines) vs. full NNLO (solid lines). Left plot ($\hat{s} \in [0, 0.05]$): lower most curves are for $\mu = 10$ GeV, uppermost ones for $\mu = 2.5$ GeV. Right plot: μ dependence reversed

- **Scale-dependence in NNLO reduced**
- $\mathcal{B}(B \to X_s \ell^+ \ell^-)_{\rm NNLO} < \mathcal{B}(B \to X_s \ell^+ \ell^-)_{\rm NLO}$
- $\mathcal{B}(B \to X_s e^+ e^-) = (6.9 \pm 0.7) \times 10^{-6}$

  $\mathcal{B}(B \to X_s \mu^+ \mu^-) = (4.15 \pm 1.0) \times 10^{-6}$

$B \to X_s \ell^+ \ell^-$ distributions

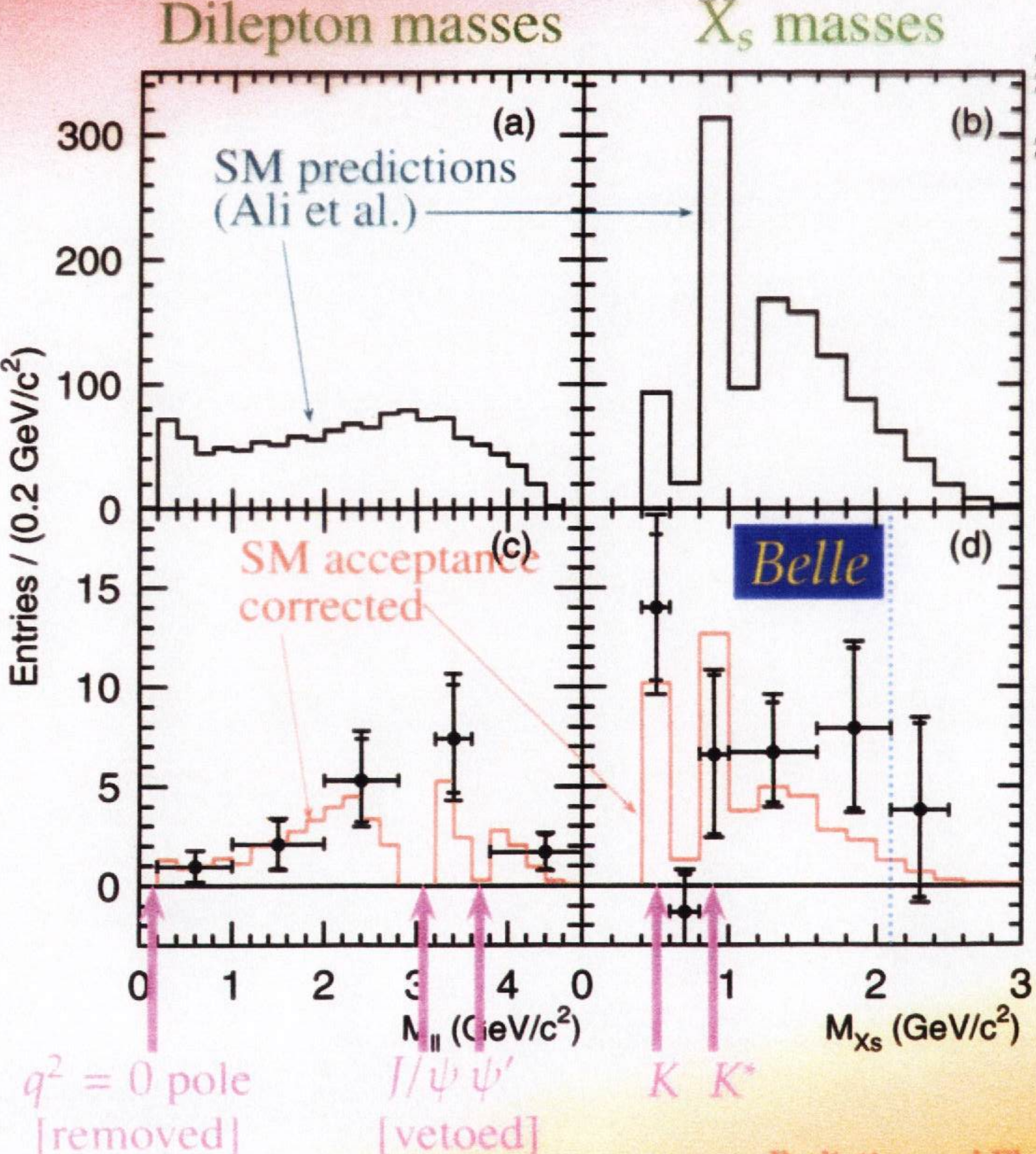

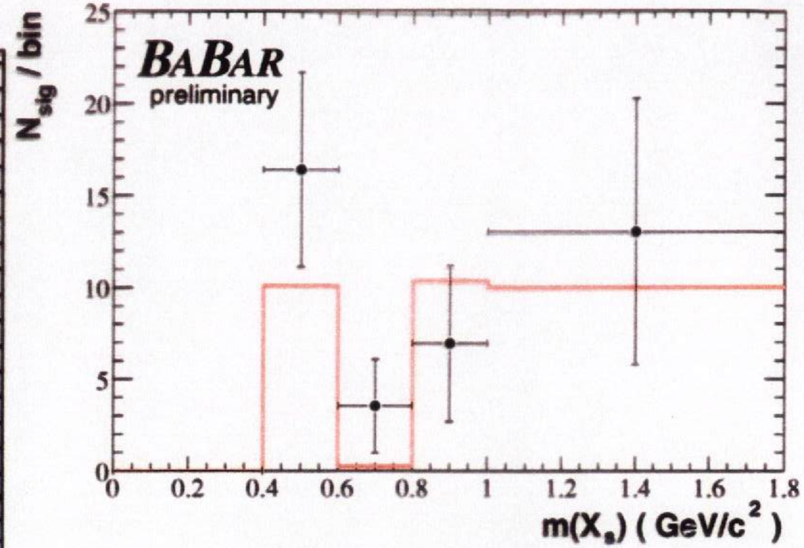

- From bin-by-bin fit to M_{bc}
- No deviation from expectation so far
- With more data, one can perform A_{FB} measuremts

$B \to X_s \ell^+ \ell^-$ branching fraction

	$B \to X_s \ell^+ \ell^-$ combined
Belle	$(6.1 \pm 1.4 ^{+1.4}_{-1.1}) \times 10^{-6}$ (5.4σ)
BaBar	$(6.3 \pm 1.6 ^{+1.8}_{-1.5}) \times 10^{-6}$ (4.6σ)
Average [MN]	$\mathbf{(6.2 \pm 1.1 ^{+1.6}_{-1.3}) \times 10^{-6}}$

(MN: simple systematic error average assuming 100% correlation)

- SM predicts $\mathcal{B} = (4.2 \pm 0.7) \times 10^{-6}$ for both $B \to X_s e^+ e^-$ and $B \to X_s \mu^+ \mu^-$ when the $q^2 = 0$ pole is removed ($M(\ell^+\ell^-) > 0.2$ GeV)
- Reasonable agreement with SM (only 1σ off, error is still large) New result will further constrain the Wilson coefficients C_9 and C_{10}

Breakdown	$B \to X_s e^+ e^-$	$B \to X_s \mu^+ \mu^-$
Belle	$(5.0 \pm 2.3 ^{+1.3}_{-1.1}) \times 10^{-6}$ (3.4σ)	$(7.9 \pm 2.1 ^{+2.1}_{-1.5}) \times 10^{-6}$ (4.7σ)
BaBar	$(6.6 \pm 1.9 ^{+1.9}_{-1.6}) \times 10^{-6}$ (4.0σ)	$(5.7 \pm 2.8 ^{+1.7}_{-1.4}) \times 10^{-6}$ (2.2σ)

NNLL-Forward-Backward Asymmetry in $B \to X_s \ell^+ \ell^-$

[H.Asatrian, K. Bieri, C. Greub, A. Hovhannisyan; hep-ph/0209006;
A. Ghinculov, T. Hurth, G. Isidori, Y.-P. Yao; hep-ph/0208088]

Normalized FB Asymmetry

$$\overline{A}_{\rm FB}(\hat{s}) = \frac{\int_{-1}^{1} \frac{d^2\Gamma(b\to X_s\,\ell^+\ell^-)}{d\hat{s}\,dz}\,\mathbf{sgn}(z)\,dz}{\int_{-1}^{1} \frac{d^2\Gamma(b\to X_s\,\ell^+\ell^-)}{d\hat{s}\,dz}\,dz}$$

Unnormalized FB Asymmetry

$$A_{\rm FB}(\hat{s}) = \frac{\int_{-1}^{1} \frac{d^2\Gamma(b\to X_s\,\ell^+\ell^-)}{d\hat{s}\,dz}\,\mathbf{sgn}(z)\,dz}{\Gamma(B\to X_c e\bar{\nu}_e)}\,\mathbf{BR}_{\rm sl}$$

$$\int_{-1}^{1} \frac{d^2\Gamma(b\to X_s\,\ell^+\ell^-)}{d\hat{s}\,dz}\,\mathbf{sgn}(z)\,dz = \left(\frac{\alpha_{\rm em}}{4\,\pi}\right)^2 \frac{G_F^2\, m_{b,\rm pole}^5 \left|V_{ts}^* V_{tb}\right|^2}{48\,\pi^3}(1-\hat{s})^2$$

$$\times \left[-3\,\hat{s}\,\mathbf{Re}(\widetilde{C}_9^{\rm eff}\widetilde{C}_{10}^{\rm eff*})\left(1+\frac{2\alpha_s}{\pi}\,f_{910}(\hat{s})\right) - 6\,\mathbf{Re}(\widetilde{C}_7^{\rm eff}\widetilde{C}_{10}^{\rm eff*})\left(1+\frac{2\alpha_s}{\pi}\,f_7\right.\right.$$

- **NNLL Contributions stabilize the scale ($=\mu$) dependence of the FB Asymmetry; Residual (small) parametric dependence dominated by $\delta(m_c/m_b)$**

$$A_{\rm FB}^{\rm NLL}(0) = -(2.51 \pm 0.28)\times 10^{-6}; \quad A_{\rm FB}^{\rm NNLL}(0) = -(2.30 \pm 0.10)\times 10^{-6}$$

- **Zero of the FB Asymmetry is a precise test of the SM, correlating $\widetilde{C}_7^{\rm eff}$ and $\widetilde{C}_9^{\rm eff}$; NNLL Corrections $\Longrightarrow$ shift in $\hat{s}_0^{\rm NLL}$**

$$\hat{s}_0^{\rm NLL} = 0.144 \pm 0.020; \quad \hat{s}_0^{\rm NNLL} = 0.162 \pm 0.008$$

FB Asymmetry in $B \to X_s \ell^+ \ell^-$

Asatrian et al.
hep-ph/0209006

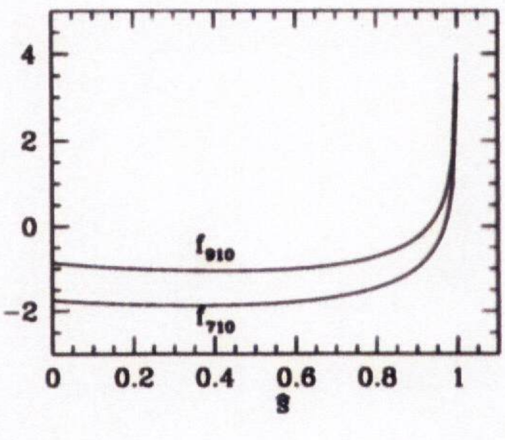

μ-dependence

$A_{FB}(\hat{s})$ $\bar{A}_{FB}(\hat{s})$

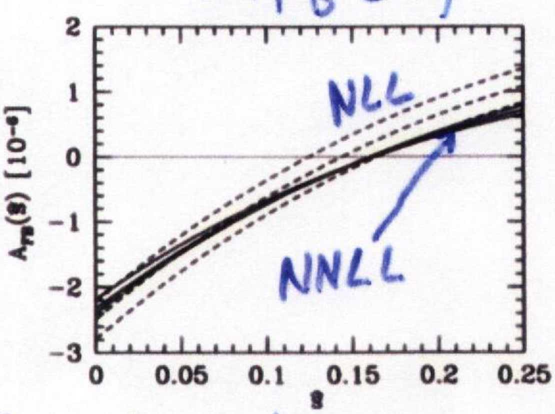

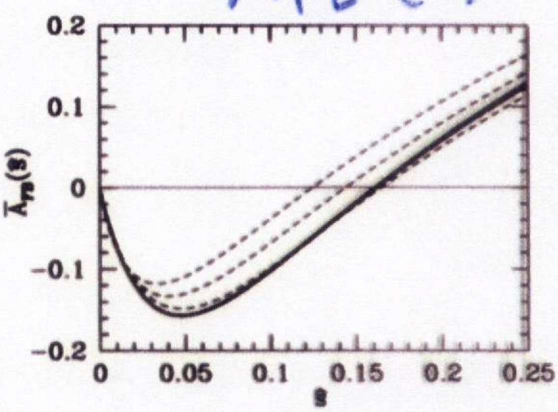

m_c/m_b-dependence

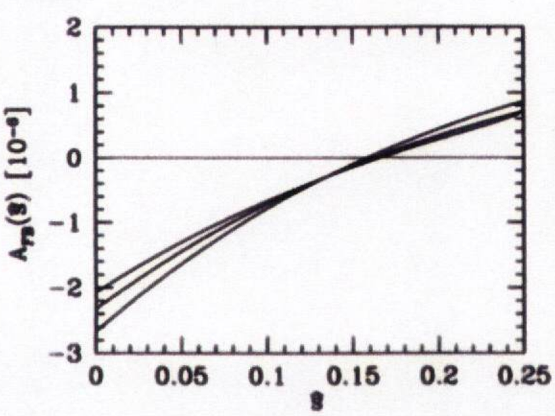

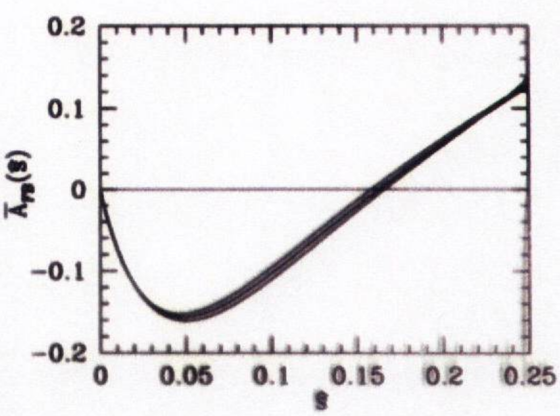

[A.A., Lunghi, Greub, Hiller; DESY 01-217; hep-ph/0112300]

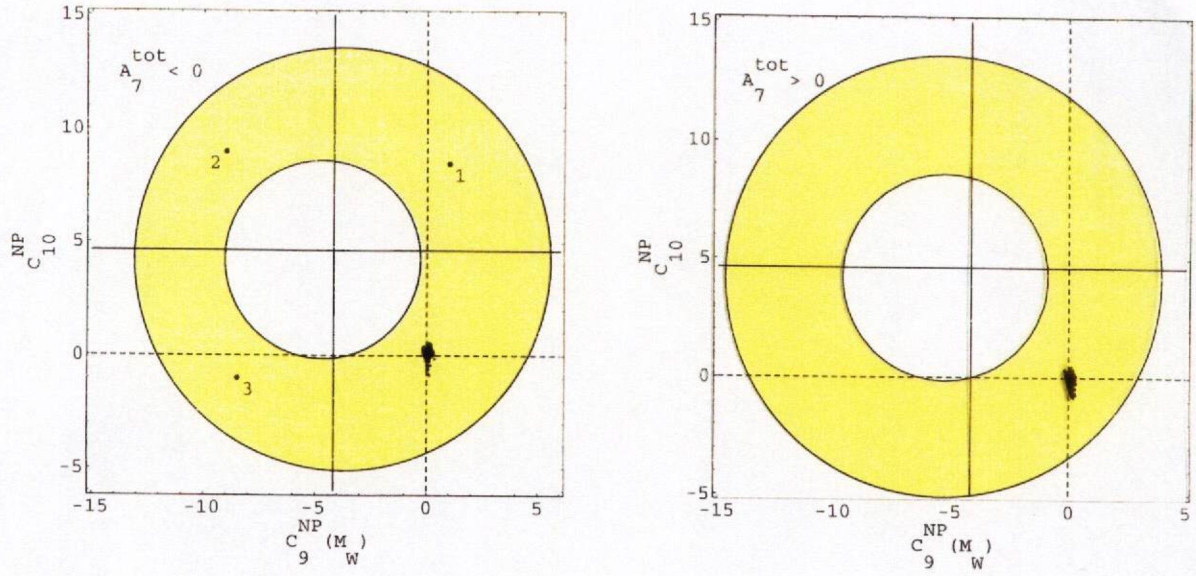

Figure 7: NNLO Case. Superposition of all the constraints from radiative and semileptonic rare decays (Points refer to the SUSY-MFV Model)

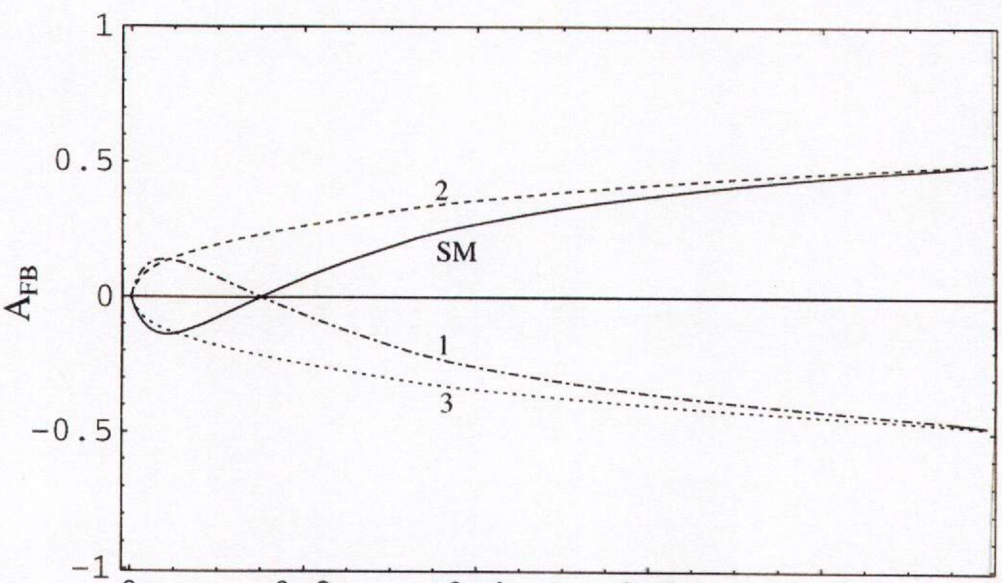

Figure 8: Differential Forward–Backward asymmetry for $B \to X_s \ell^+ \ell^-$. The four curves correspond to the points indicated above

Exclusive Decays $B \to (K, K^*)\ell^+\ell^-$

- $B \to K$ **(pseudoscalar** P**);** $B \to K^*$ **(Vector** V**) Transitions involve the currents:**

$$\Gamma_\mu^1 = s\gamma_\mu(1 - \gamma_5)b, \quad \Gamma_\mu^2 = s\sigma_{\mu\nu}q^\nu(1 + \gamma_5)b$$

$$\langle P|\Gamma_\mu^1|B\rangle \supset f_+(q^2), f_-(q^2)$$

$$\langle P|\Gamma_\mu^2|B\rangle \supset f_T(q^2)$$

$$\langle V|\Gamma_\mu^1|B\rangle \supset V(q^2), A_1(q^2), A_2(q^2), A_3(q^2)$$

$$\langle V|\Gamma_\mu^2|B\rangle \supset T_1(q^2), T_2(q^2), T_3(q^2)$$

- **10 non-perturbative** q^2**-dependent functions (Form factors)** $\Longrightarrow$ **model-dependence**

- **Data on** $B \to K^*\gamma$ **provides normalization of** $T_1(0) = T_2(0) \simeq 0.28$

- **HQET/LEET-Approach allows to reduce the number of independent form factors from 10 to 3; perturbative symmetry-breaking corrections** [Beneke, Feldmann, Seidel; Beneke, Feldmann]

- **HQET & SU(3) relate** $B \to (\pi, \rho)\ell\nu_\ell$ **and** $B \to (K, K^*)\ell^+\ell^-$ **to determine the remaining FF's**

- **Need good measurements of the decays** $B \to (\pi, \rho)\ell\nu_\ell$ **and** V_{ub} **to make model-independent predictions for the decays** $B \to (K, K^*)\ell^+\ell^-$

$B \to (K^*, \rho)\gamma$ Decay Rates in NLO

- Large Energy Effective Theory (LEET)
  [Dugan, Grinstein '91; Charles et al. '99]
  $$E_V = \frac{m_B}{2}\left(1 - \frac{q^2}{m_B^2} + \frac{m_V^2}{m_B^2}\right)$$
  For Large $E_V \sim m_B/2$, i.e., $q^2/m_B^2 \ll 1$; Symmetries in the Effective Theory $\Longrightarrow$ Relations among FFs:
  $$f_k(q^2) = C_{\perp k}\xi_\perp(q^2) + C_{\parallel k}\xi_\parallel(q^2)$$
- LEET-symmetries broken by perturbation theory
  Factorization Ansatz:
  [Beneke, Buchalla, Neubert, Sachrajda; Beneke & Feldmann]
  $$f_k(q^2) = C_{\perp k}\xi_\perp(q^2) + C_{\parallel k}\xi_\parallel(q^2) + \Phi_B \otimes T_k \otimes \Phi_V$$
  Perturbative Corrections:
  $$C_i = C_i^{(0)} + \frac{\alpha_s}{\pi} C_i^{(1)} + \ldots$$
- T_k: Hard Spectator Corrections
  $$\Delta\mathcal{M}^{(\mathrm{HSA})} = \frac{4\pi\alpha_s C_F}{N_c}\int_0^1 du \int_0^\infty dl_+\, M_{jk}^{(B)} M_{li}^{(V)} \mathcal{T}_{ijkl},$$
- $M_{jk}^{(B)}$ and $M_{li}^{(V)}$ B-Meson & V-Meson Projection Operators

Symmetry in the Large Energy Limit & FFs in $B \to K^* \ell^+ \ell^-$

$$
\begin{aligned}
A_0(s) &= (1 - \frac{m_V^2}{m_B E_V})\, \xi_{||}(s) + \frac{m_V}{m_B}\, \xi_\perp(s) \\
A_1(s) &= \frac{2E_V}{m_B + m_V}\, \xi_\perp(s)\ , \\
A_2(s) &= (1 + \frac{m_V}{m_B})\, [\, \xi_\perp(s) - \frac{m_V}{E_V}\, \xi_{||}(s)\,] \\
V(s) &= (1 + \frac{m_V}{m_B})\, \xi_\perp(s) \\
T_1(s) &= \xi_\perp(s) \\
T_2(s) &= (1 - \frac{s}{m_B^2 - m_V^2})\, \xi_\perp(s) \\
T_3(s) &= \xi_\perp(s) - \frac{m_V}{E_V}\, (1 - \frac{m_V^2}{m_B^2})\, \xi_{||}(s)
\end{aligned}
$$

where

$$
E_V = \frac{m_B}{2}\left(1 - \frac{s}{m_B^2} + \frac{m_V^2}{m_B^2}\right)
$$

- In the symmetry limit, only two FFs: $\xi_\perp(s)$ & $\xi_{||}(s)$
- Normalization of $\xi_\perp(0)$ from $B \to K^* \gamma$
- Use LC-QCD Sum Rules for parametrizing $\xi_\perp(s)$ & $\xi_{||}(s)$

Perturbative QCD corrections in $B \to K^* \ell^+ \ell^-$

[Beneke, Feldmann; Beneke, Feldmann, Seidel]

$$
\begin{aligned}
A_1(s) &= \frac{2E_V}{m_B + m_V}\, \xi_\perp(s) + \frac{\alpha_s C_F}{4\pi}\, \Delta A_1 \\
A_2(s) &= \frac{m_B}{m_B - m_V}\left[\xi_\perp(s) - \frac{m_V}{E_V}\, \xi_{||}(s)(1 + \frac{\alpha_s C_F}{4\pi}[-2 + 2L])\right] \\
&+ \frac{\alpha_s C_F}{4\pi}\, \Delta A_2
\end{aligned}
$$

with

$$
\begin{aligned}
L &= -\frac{2E_V}{m_B - 2E_V}\, \ln \frac{2E_V}{m_B} \\
\Delta A_1 = 0,\ \Delta A_2 &= \frac{m_V}{m_B - m_V}\, \frac{m_B^2(m_B - 2E_V)}{4E_V^3} \Delta F_{||} \\
\Delta F_{||} &= \frac{8\pi^2 f_B f_V}{N_C m_B} \langle \ell_+^{-1} \rangle_+ \langle \bar{u}^{-1} \rangle_{||}
\end{aligned}
$$

Dilepton Invariant Mass Distribution for $B \to K^* \ell^+ \ell^-$

- For $m_\ell = 0$, no contribution from the FF $A_0(\hat{s})$
- Enhancement in dilepton mass spectrum in low $\hat{s}$-region due to the dependence $\frac{d\Gamma}{d\hat{s}} \sim C_7^{eff^2}/\hat{s}$; photon pole cotribution dominant for $q^2 < 1$ GeV^2 $\Longrightarrow \mathcal{B}(B \to K^* e^+ e^-) > \mathcal{B}(B \to K^* \mu^+ \mu^-)$
- Like $B \to K \ell^+ \ell^-$, following combinations of WC's are involved: $|C_{10}|^2, \; |C_9|^2, \; |C_7^{eff}|^2, \; Re(C_7^{eff} C_9^{eff})$
- HQET/LEET can be used advantageously to reduce the number of independent form factors to 2; $O(\alpha_s)$-corrections to the HQET/LEET symmetry calculated [Beneke, Feldmann; Beneke, Feldmann, Seidel]
- Residual FF-related uncertainties can be reduced by relating $B \to K^* \ell^+ \ell^-$ with $B \to \rho \ell \nu_\ell$ and SU(3)-breaking; Data on $B \to \rho \ell \nu_\ell$ not yet precise enough to warrant this analysis
- Helicity analysis of $B \to K^* \ell^+ \ell^-$ in terms of the components $H_+(\hat{s}), H_-(\hat{s})$ and $H_0(\hat{s})$ and using data on $B \to K^* \gamma \Longrightarrow$ rather precise dilepton mass spectrum for the $H_-(\hat{s})$ component [Safir, AA '02]
- SM estimates (in NNLO) [AA, Lunghi, Greub, Hiller '01]:

$$\mathcal{B}(B \to K^* e^+ e^-) = (1.58 \pm 0.52) \times 10^{-6}$$
$$\mathcal{B}(B \to K^* \mu^+ \mu^-) = (1.2 \pm 0.4) \times 10^{-6}$$

- $\mathcal{B}(B \to K^* \ell^+ \ell^-)$ and $\mathcal{B}(B \to \rho \ell^+ \ell^-)$ can be used (like $B \to (K, \pi) \ell^+ \ell^-$) to determine the CKM matrix elements $|V_{ts}|$ and $|V_{td}|$
- Sizable distrotion of the dilepton spectrum allowed in New Physics scenarios, such as supersymmetry

Dilepton Invariant Mass Distribution for $B \to K\ell^+\ell^-$

$$\frac{d\Gamma}{d\hat{s}} = |V_{ts}^* V_{tb}|^2 (|C_9^{eff} f_+ + \frac{2\hat{m}_b}{1+\hat{m}_K} C_7^{eff} f_T|^2 + |C_{10} f_+|^2)$$

- For $m_\ell = 0$, no contribution from the FF f_-
- In SM, $|C_7^{eff}| \ll |C_9^{eff}, C_{10}$, and no kinematical enhancement at low $\hat{s}$ (as opposed to $B \to K^*\ell^+\ell^-$); To a good approximation ($O(10\%)$)

$$\frac{d\Gamma}{d\hat{s}} \sim |f_+(\hat{s})|^2$$

- $f_+(\hat{s})$ determined from $B \to \pi\ell\nu_\ell$ and SU(3)-breaking

Constraints on the CKM Matrix Elements

- $\mathcal{B}(B \to K\ell^+\ell^-) \implies$ a determination of $|V_{ub}/V_{ts}^* V_{tb}|$ [Ligeti, Stewart, Wise]
- $\mathcal{B}(B \to \pi\ell^+\ell^-) \implies$ a precise determination of $|V_{ub}/V_{td}^* V_{tb}|$
- SM estimates (in NNLO) [AA, Lunghi, Greub, Hiller '01]:

$$\mathcal{B}(B \to K\ell^+\ell^-) = (0.35 \pm 0.12) \times 10^{-6}$$
$$\mathcal{B}(B \to \pi\ell^+\ell^-) = (0.24 \pm 0.10) \times |\frac{V_{td}}{V_{ts}}|^2 \times 10^{-6} \simeq 10^{-8}$$

Sensitivity to New Physics

- $B \to X_s\gamma$ Data implies $|C_7^{eff}| \simeq |C_7^{eff}(\mathrm{SM})| \implies$ Two possible solutions
- $C_7^{eff} \simeq C_7^{eff}(\mathrm{SM})$; (SUGRA-type solutions for low $\tan\beta$); hard to distinguish from SM
- $C_7^{eff} \simeq -C_7^{eff}(\mathrm{SM})$; (allowed solution in SUGRA-type models with large $\tan\beta$); distinguishable through a precise measurement of the dilepton mass spectrum [Okada et al.; AA, Ball, Handoko, Hiller]

Dilepton inv. mass distribution Ball, Handoko, Hiller, A.-A. hep-ph/9910221

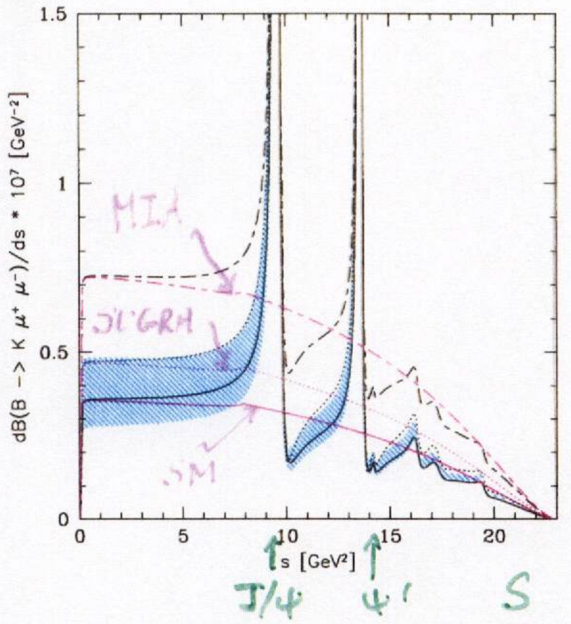

Figure 6: *The dilepton invariant mass distribution in $B \to K\mu^+\mu^-$ decays, using the form factors from LCSR as a function of s. All resonant $c\bar{c}$ states are parametrized as in Ref. [29]. The solid line represents the SM and the shaded area depicts the form factor-related uncertainties. The dotted line corresponds to the SUGRA model with $R_7 = -1.2$, $R_9 = 1.03$ and $R_{10} = 1$. The long-short dashed lines correspond to an allowed point in the parameter space of the MIA-SUSY model, given by $R_7 = -0.83$, $R_9 = 0.92$ and $R_{10} = 1.61$. The corresponding pure SD spectra are shown in the lower part of the plot.*

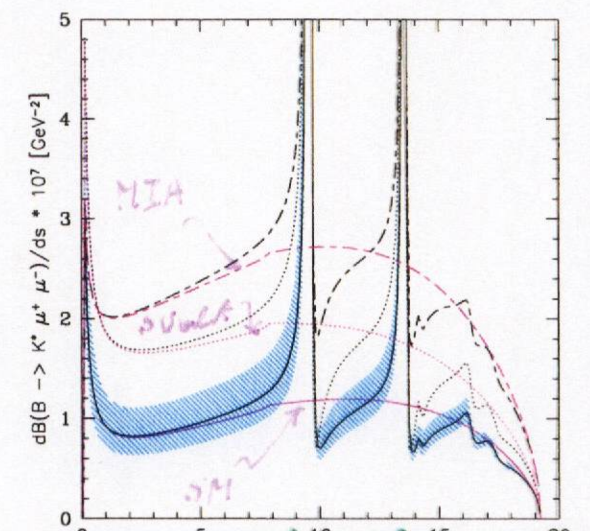

Figure 7: *The dilepton invariant mass distribution in $B \to K^*\mu^+\mu^-$ decays, using the form factors from LCSR as a function of s. All resonant $c\bar{c}$ states are parametrized as in Ref. [29]. The legends are the same as in Fig. 6.*

$B \to K^{(*)}\ell^+\ell^-$ distributions

BaBar's $M(\ell^+\ell^-)$, compared with SM

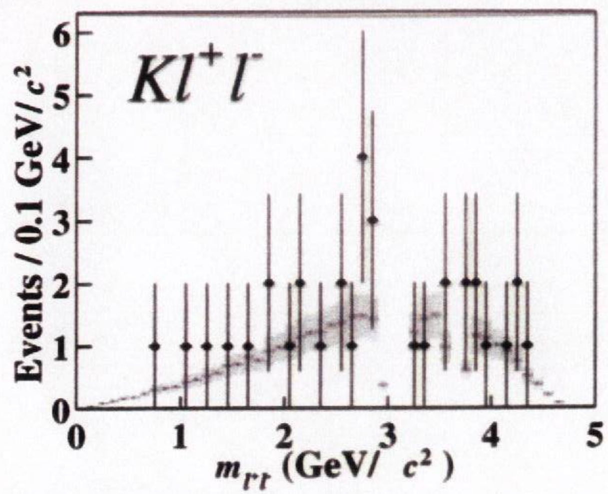

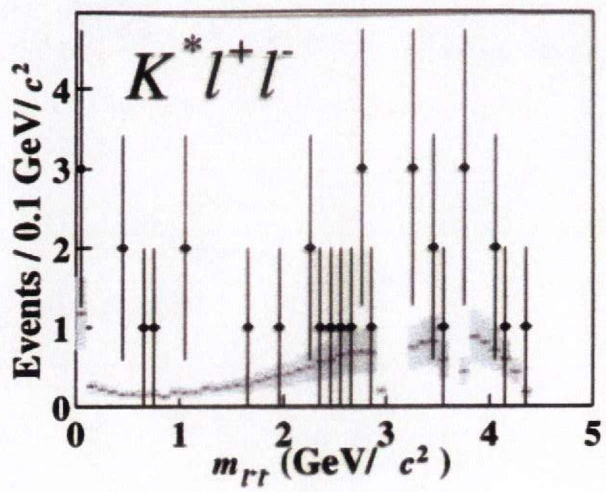

Belle's q^2 distributions from bin-by-bin fit to M_{bc} ($q^2 = M(\ell^+\ell^-)^2$)

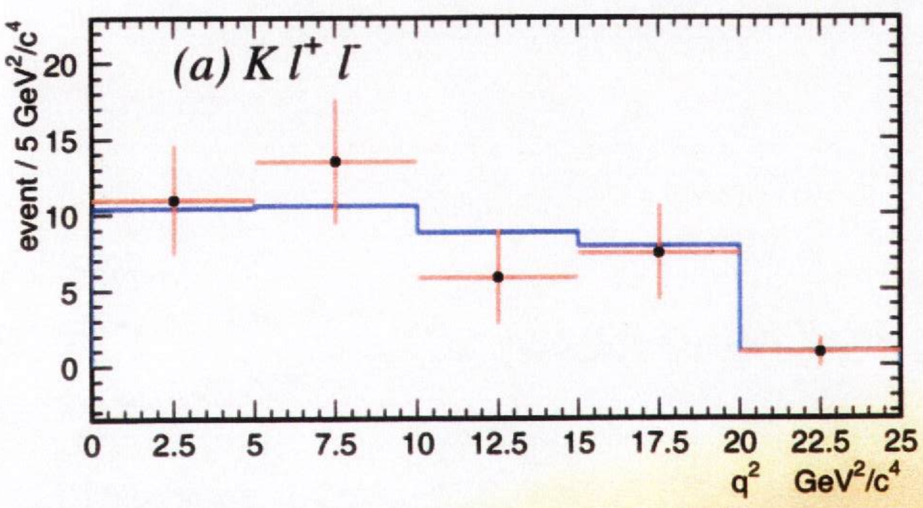

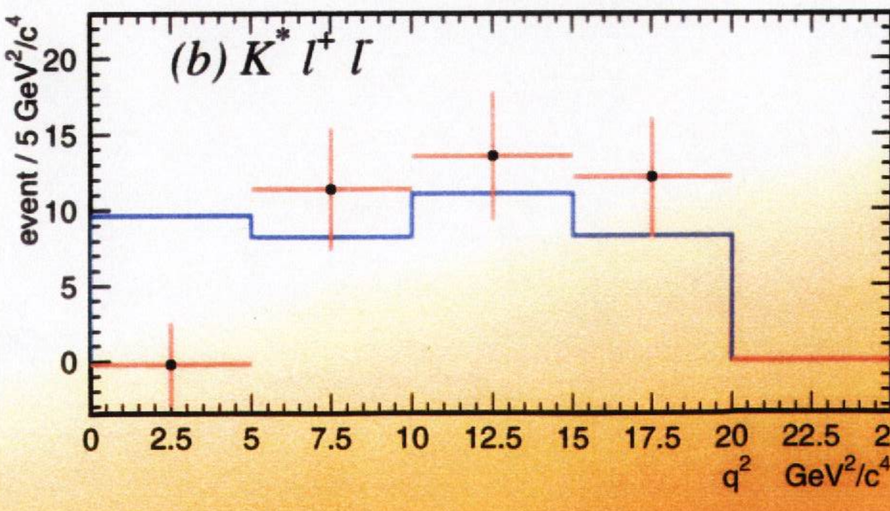

$B \to K^{(*)}\ell^+\ell^-$ branching fractions

Mode	Belle $\mathcal{B} \pm$ stat $\pm$ syst $\pm$ model	BaBar $\mathcal{B} \pm$ stat $\pm$ syst
$B \to Ke^+e^-$	$(4.8^{+1.5}_{-1.3} \pm 0.3 \pm 0.1) \times 10^{-7}$	$(7.9^{+1.9}_{-1.7} \pm 0.7) \times 10^{-7}$
$B \to K\mu^+\mu^-$	$(4.8^{+1.3}_{-1.1} \pm 0.3 \pm 0.2) \times 10^{-7}$	$(4.8^{+2.5}_{-2.0} \pm 0.4) \times 10^{-7}$
$B \to K\ell^+\ell^-$	$(4.8^{+1.0}_{-0.9} \pm 0.3 \pm 0.1) \times 10^{-7}$	$(6.9^{+1.5}_{-1.3} \pm 0.6) \times 10^{-7}$

SM: $\mathcal{B}(B \to K\ell^+\ell^-) = (3.5 \pm 1.2) \times 10^{-7}$

$B \to K^*e^+e^-$	$(14.9^{+5.2}_{-4.6}{}^{+1.1}_{-1.3} \pm 0.3) \times 10^{-7}$	$(10.0^{+5.0}_{-4.2} \pm 1.3) \times 10^{-7}$
$B \to K^*\mu^+\mu^-$	$(11.7^{+3.6}_{-3.1} \pm 0.8 \pm 0.6) \times 10^{-7}$	$(12.8^{+7.8}_{-6.2} \pm 1.7) \times 10^{-7}$
$B \to K^*\ell^+\ell^-$	$(11.5^{+2.6}_{-2.4} \pm 0.7 \pm 0.4) \times 10^{-7}$	$(8.9^{+3.4}_{-2.9} \pm 1.1) \times 10^{-7}$

SM: $\mathcal{B}(B \to K^*\ell^+\ell^-) = (11.9 \pm 3.9) \times 10^{-7}$

- $\mathcal{B}(B \to K^*\ell^+\ell^-) \equiv \mathcal{B}(B \to K^*\mu^+\mu^-) = 0.75 \times \mathcal{B}(B \to K^*e^+e^-)$ is assumed to compensate $q^2 = 0$ pole in e^+e^-

  (Factor 0.75, and all SM numbers are from Ali et al.)

Caution: available exclusive predictions vary by a factor of ~ 2

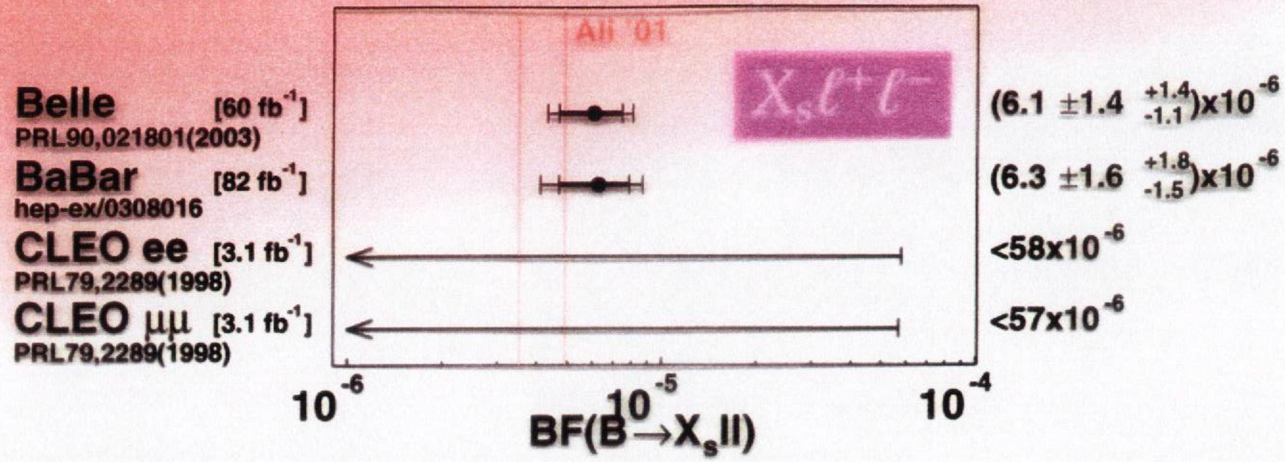

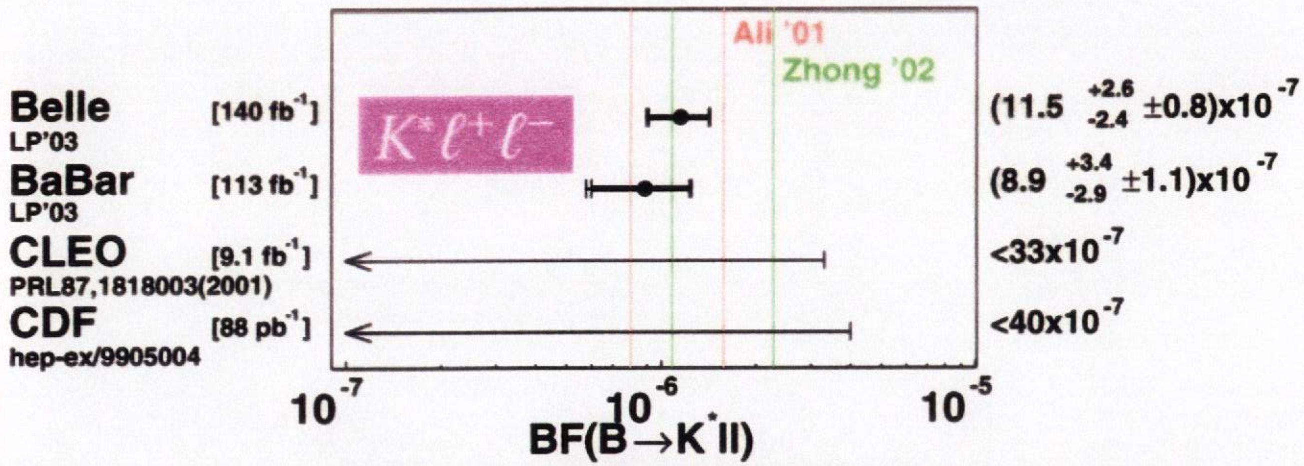

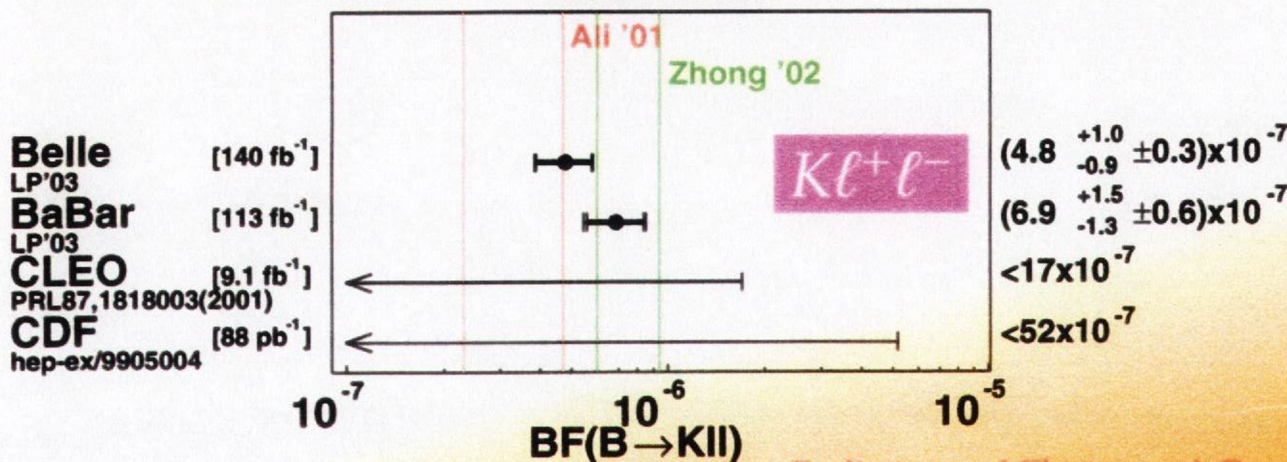

Mission completed!

$K^{(*)}\ell^+\ell^-$ and $X_s\ell^+\ell^-$ are all measured

next target:
Precise $X_s\ell^+\ell^-$,
q^2 and A_{FB}

SM predictions at NNLO accuracy & Comparison with Data

(in units of 10^{-6})

SM: [A.A., Lunghi, Greub, Hiller, DESY 01-217; hep-ph/0112300]

Experiment: HFAG (Summer 2003)

Decay Mode	Theory (SM)	Expt. (BELLE & BABAR)
$B \to K\ell^+\ell^-$	0.35 ± 0.12	0.55 ± 0.08
$B \to K^* e^+ e^-$	1.58 ± 0.52	1.25 ± 0.39
$B \to K^* \mu^+ \mu^-$	1.2 ± 0.4	1.19 ± 0.31
$B \to X_s \mu^+ \mu^-$	4.15 ± 0.70	7.0 ± 2.1
$B \to X_s e^+ e^-$	4.2 ± 0.70	5.8 ± 1.8
$B \to X_s \ell^+ \ell^-$	4.18 ± 0.70	6.2 ± 1.5

- Inclusive measurements and the SM rates include a cut $M_{\ell^+\ell^-} > 0.2$ GeV

A Model-independent Analysis of $B \to X_s\gamma$ & $B \to X_s\ell^+\ell$

- **Assume $\mathcal{H}_{eff}^{\rm SM}$ a sufficient operator basis also for Beyond-the-SM physics**

- **Shifts due to Beyond-the-SM [BSM] physics only in $C_7(\mu_W)$,$C_8(\mu_W)$, $C_9(\mu_W)$, and $C_{10}(\mu_W)$**

- **BSM Coefficients: $R_7 - 1$, $R_8 - 1$, $C_9^{\rm NP}$, & $C_{10}^{\rm NP}$**

- **Define:**

$$R_{7,8}(\mu_W) \equiv \frac{C_{7,8}^{\rm tot}(\mu_W)}{C_{7,8}^{\rm SM}(\mu_W)}$$

  with $C_{7,8}^{\rm tot}(\mu_W) = C_{7,8}^{\rm SM}(\mu_W) + C_{7,8}^{\rm NP}(\mu_W)$

- **Set the scale $\mu_W = M_W$, and use RGE to evolve**
  $R_{7,8}(\mu_W) \to R_{7,8}(\mu_b) = \frac{A_{7,8}^{\rm tot}(\mu_b)}{A_{7,8}^{\rm SM}(\mu_b)}$

- **RGE $\Longrightarrow$ modificications in $\tilde{C}_7^{eff}$, $\tilde{C}_9^{eff}$, $\tilde{C}_{10}^{eff}$**

- **Impose constraints from $R_7(\mu_b)$ and $R_8(\mu_b)$ from $B \to X_s\gamma$ Data**

- **Use Data on $B \to (X_s, K^*, K)\ell^+\ell^-$ BRs to constrain $C_9^{\rm NP}$ and $C_{10}^{\rm NP}$**

- **Two-fold ambiguity due to the sign of C_7^{eff}**
  $\Longrightarrow$ Two-fold ambiguity for $C_9^{\rm NP}$ and $C_{10}^{\rm NP}$

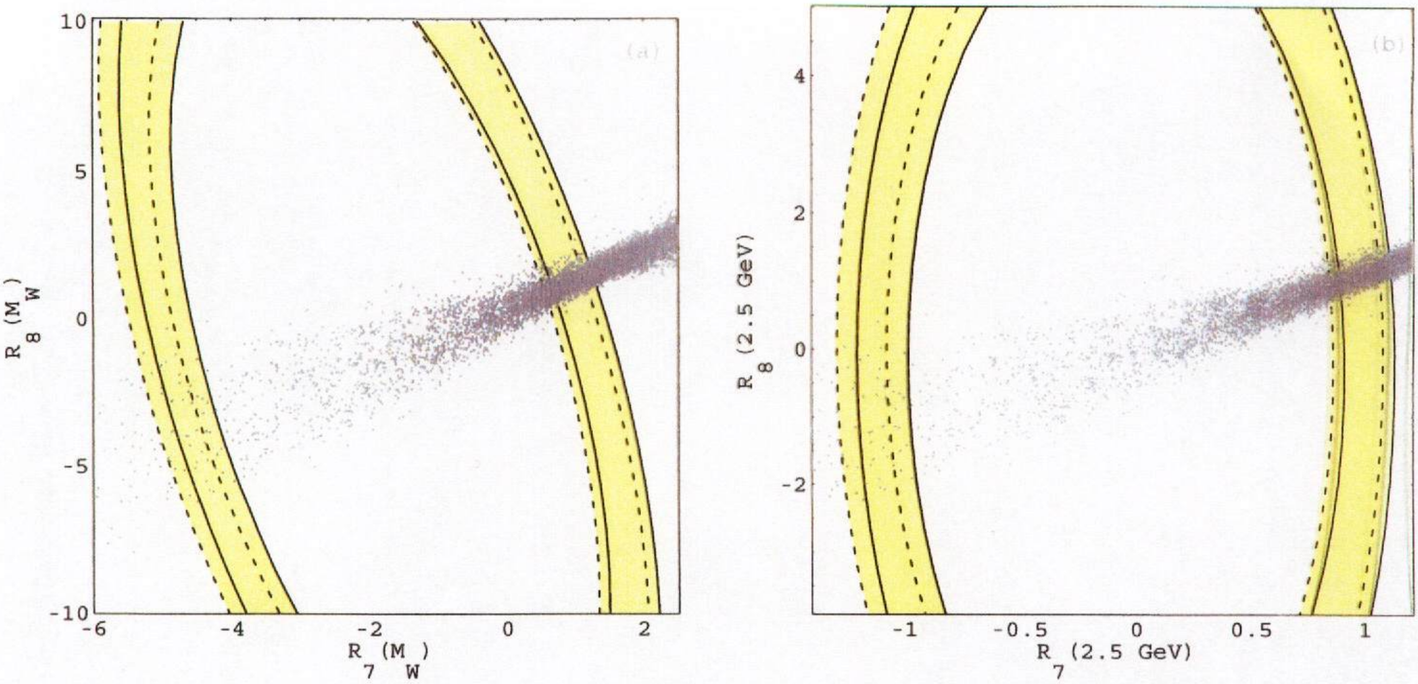

Figure 7: 90% C.L. **bounds in the** $[R_7(\mu), R_8(\mu)]$ **plane from the** $\mathcal{B}(B \to X_s\gamma)$ **for two choices of** m_c/m_b**.** $\mu = m_W$ **(left-hand plot) and** $\mu = 2.5$ **GeV (right-hand plot). The scattered points are generated in the SUSY-MFV model.**

$$\begin{cases} m_c/m_b = 0.29: & A_7^{\rm tot}(2.5\ \textbf{GeV}) \in [-0.37, -0.18]\ \&\ [0.21, 0.40]\,, \\ m_c/m_b = 0.22: & A_7^{\rm tot}(2.5\ \textbf{GeV}) \in [-0.35, -0.17]\ \&\ [0.25, 0.43]\,. \end{cases}$$

$\Longrightarrow$

$$A_7^{\rm tot} - \text{negative}: -0.37 \le A_7^{\rm tot,<0}(2.5\ \textbf{GeV}) \le -0.17$$
$$A_7^{\rm tot} - \text{positive}: 0.21 \le A_7^{\rm tot,>0}(2.5\ \textbf{GeV}) \le 0.43$$

- Data allows a larger range for $R_8(2.5\ \mathrm{GeV})$

[A.A., Lunghi, Greub, Hiller; DESY 01-217; hep-ph/0112300]

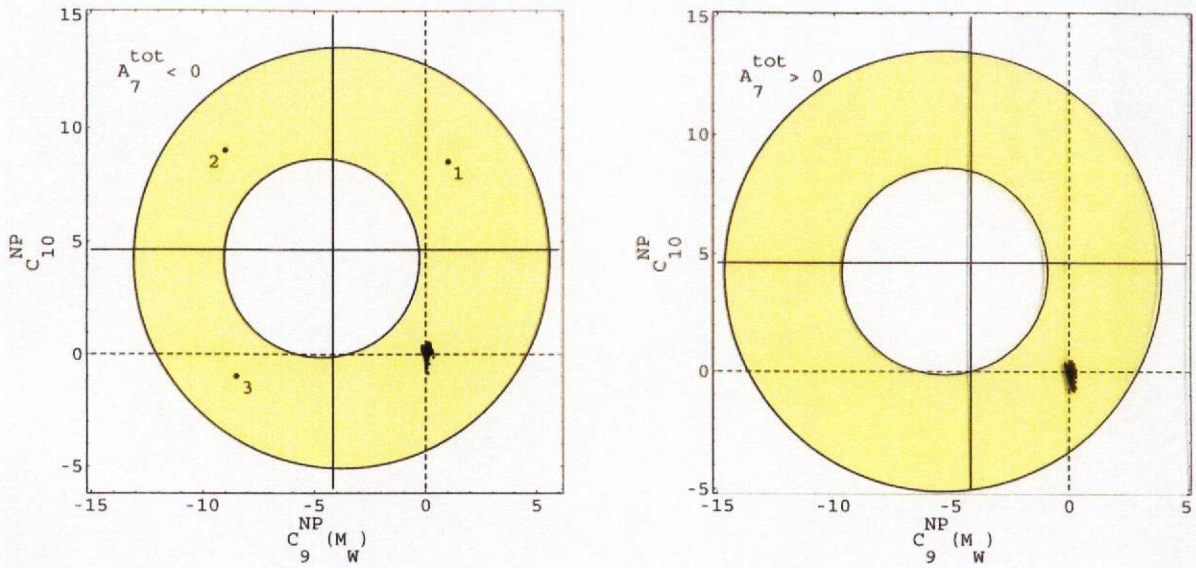

Figure 8: NNLO Case. Superposition of all the constraints from radiative and semileptonic rare decays (Points refer to the SUSY-MFV Model)

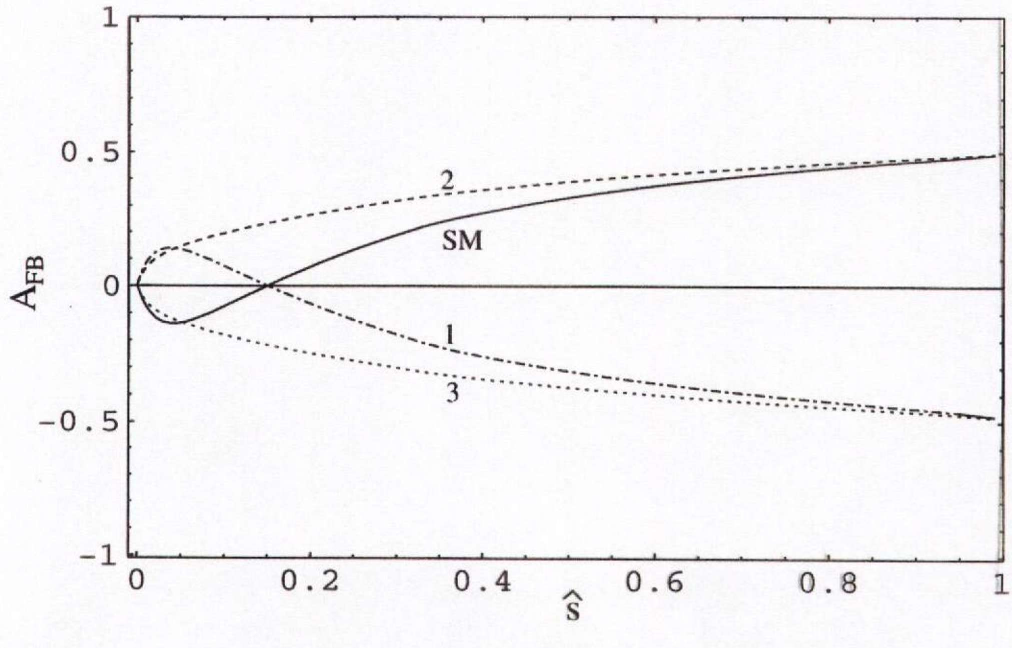

Figure 9: Differential Forward–Backward asymmetry for $B \to X_s \ell^+ \ell^-$. The four curves correspond to the points indicated above

Forward-Backward Asymmetry in $B \to K^* \ell^+ \ell^-$

$(\hat{u} \sim \cos\theta; \quad \theta = \angle(p_B, p_{\ell^+})$ in dilepton CMS

$$\frac{dA_{FB}}{d\hat{s}} = -\int_0^{\hat{u}(\hat{s})} d\hat{u} \frac{d\Gamma}{d\hat{u}d\hat{s}} + \int_{-\hat{u}(\hat{s})}^0 d\hat{u} \frac{d\Gamma}{d\hat{u}d\hat{s}}$$

$$\sim C_{10}[\mathrm{Re}(C_9^{eff}) V A_1 + \frac{\hat{m}_b}{\hat{s}} C_7^{eff} (V T_2 (1 - \hat{m}_V) + A_1 T_1 (1 + \hat{m}_V))]$$

- **Probes different combinations of WC's than dilepton mass spectrum; has a characteristic zero in the SM ($\hat{s}_0$) below $m^2_{J/\psi}$**

Position of the $A_{FB}(\hat{s})$ zero ($\hat{s}_0$) in $B \to K^* \ell^+ \ell^-$

$$\mathrm{Re}(C_9^{eff}(\hat{s}_0)) = -\frac{\hat{m}_b}{\hat{s}_0} C_7^{eff} (\frac{T_2(\hat{s}_0)}{A_1(\hat{s}_0)} (1 - \hat{m}_V) + \frac{T_1(\hat{s}_0)}{V(\hat{s}_0)} (1 + \hat{m}_V))$$

- **Model-dependent studies $\Longrightarrow$ small FF-related uncertainties in $\hat{s}_0$ [Burdman '98]**
- **HQET/LEET provide a symmetry argument why the uncertainty in $\hat{s}_0$ is small. In leading order in $1/m_B$, $1/E$ ($E = \frac{m_B^2 + m_{K^*}^2 - q^2}{2m_B}$) and $O(\alpha_s)$:**

$$\frac{T_2}{A_1} = \frac{1 + \hat{m}_V}{1 + \hat{m}_V^2 - \hat{s}} (1 - \frac{\hat{s}}{1 - \hat{m}_V^2})$$

$$\frac{T_1}{V} = \frac{1}{1 + \hat{m}_V}$$

- **No hadronic uncertainty in $\hat{s}_0$ [AA, Ball, Handoko, Hiller '99]**

$$C_9^{eff}(\hat{s}_0) = -\frac{2 m_b M_B}{s_0} C_7^{eff}$$

- $O(\alpha_s)$ **corrections to the LEET-symmetry relations lead to substantial perturbative shift in** $\hat{s}_0$ [Beneke, Feldmann, Seidel '01]

$$C_9^{eff}(\hat{s}_0) = -\frac{2m_b M_B}{s_0} C_7^{eff}(1 + \frac{\alpha_s C_F}{4\pi}[\ln \frac{m_b^2}{\mu^2} - L] + \frac{\alpha_s C_F}{4\pi} \frac{\Delta F_\perp}{\xi_\perp(s_0)})$$

AA, A.S. Safir, DESY Report '02-005 [hep-ph/02054]

H

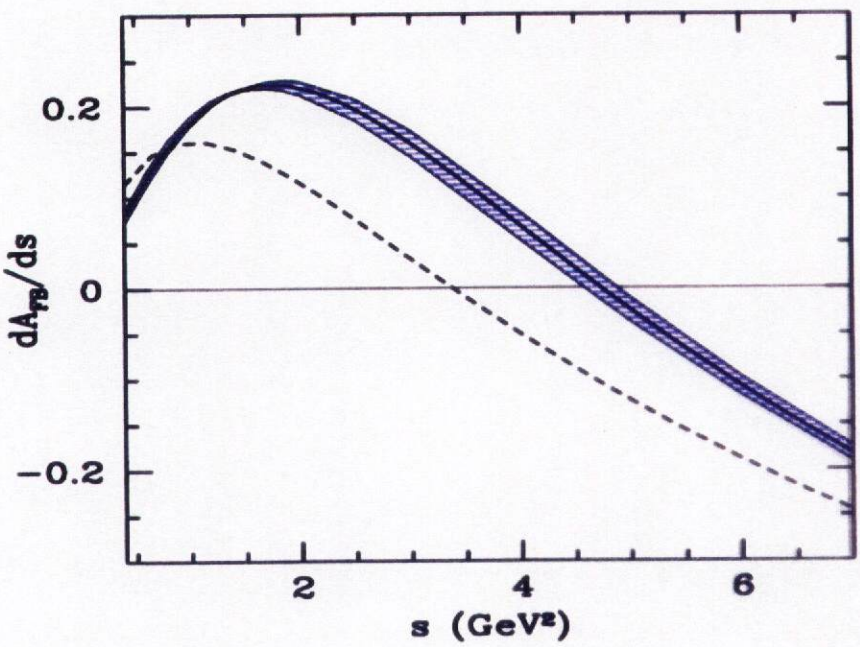

Figure 2: Forward-backward asymmetry $dA_{FB}(B \to K^* l^+ l^-)/ds$ **at next-to-leading order (solid center line) and leading order (dashed). The band reflects the theoretical uncertainties from the input parameters.**

Ball, Hiller, Handoko, …

FB Asymmetry ($B \to K^* \ell^+ \ell^-$)

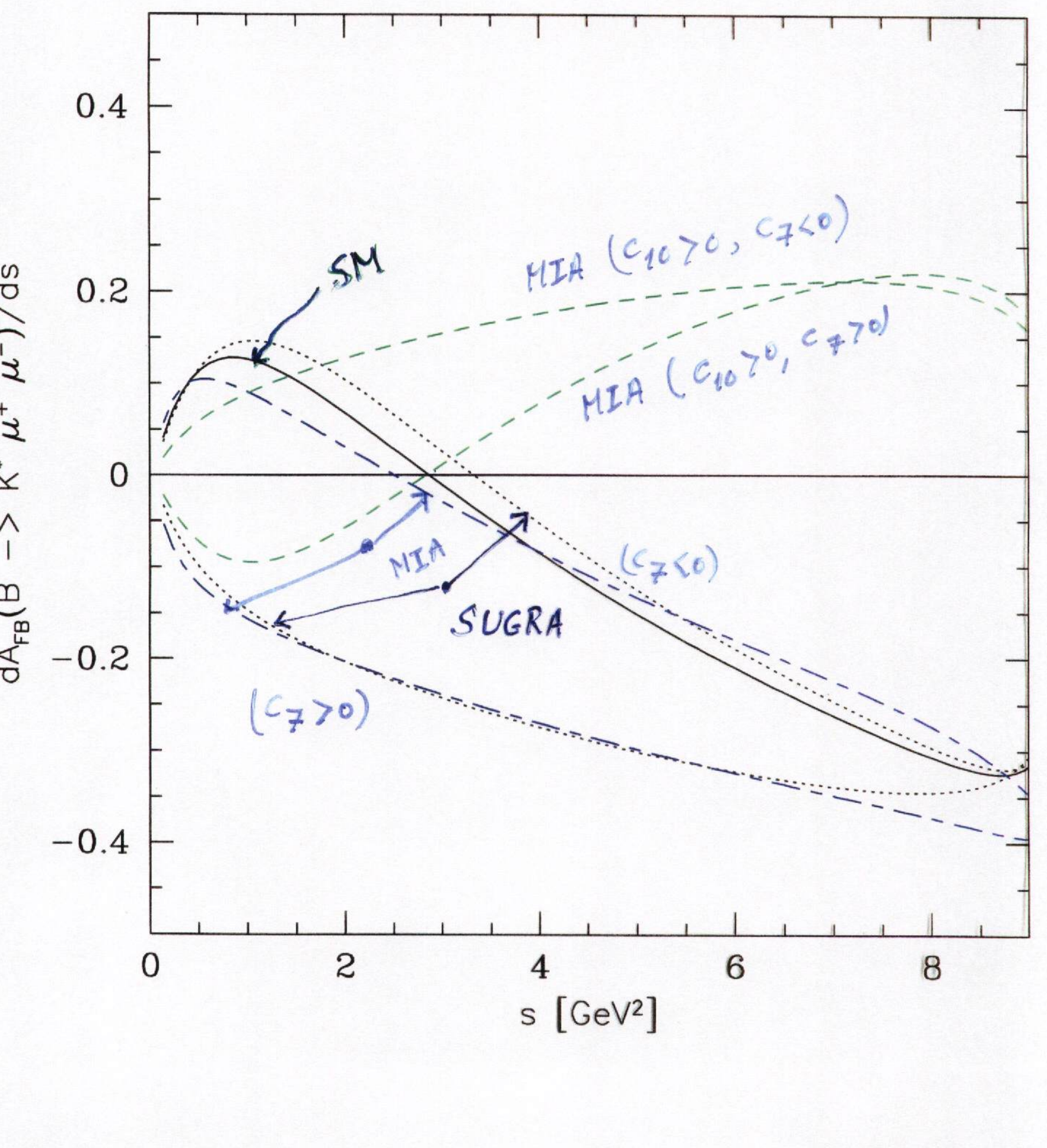

Rare Semileptonic Decays at LHCb

Source: P. Koppenburg; LHCb 2002-017

Annual Yields

$B \to \mu^+\mu^- X_s = 24200 \pm 800$	$S/B = 8.1 \pm 2.1$
$B \to \mu^+\mu^- X_d = 550 \pm 30$	$S/B = 1.3^{+0.7}_{-0.9}$
$B^\pm \to \mu^+\mu^- K^\pm = 7750 \pm 600$	$S/B = 7.3 \pm 2.0$
$B^0 \to \mu^+\mu^- K^{*0} = 8600 \pm 300$	$S/B > 15$
$B^\pm \to \mu^+\mu^- \pi^\pm = 310 \pm 20$	$S/B = 1.0^{+0.6}_{-0.7}$
$B^0 \to \mu^+\mu^- \rho^0 = 220 \pm 20$	$S/B > 2.2$

Errors on Physical Constants

$\sigma(\frac{V_{td}}{V_{ts}})/(\frac{V_{td}}{V_{ts}})$	$(11.5^{+2.8}_{-3.2})\%$ **at** $(\lvert V_{ts}\rvert/\lvert V_{td}\rvert)^2 = 30$
$\sigma(A_{\rm CP})(B \to \mu^+\mu^- X_s)$	$(2.3 \pm 0.2)\%$
$\sigma(A_{\rm FB})(B \to \mu^+\mu^- K)$	1.2% **at** $0 \le \hat{s} \le 0.32$
$\sigma(\frac{\mathcal{R}(C^{\rm eff}_{9V}(s_0))}{C^{\rm eff}_7})/\frac{\mathcal{R}(C^{\rm eff}_{9V}(s_0))}{C^{\rm eff}_7}$	$(6.0 \pm 0.3)\%$ **at** $\hat{s}_0 = 0.1307$

FB Asymmetry in $B \to \mu^+\mu^- K^*$

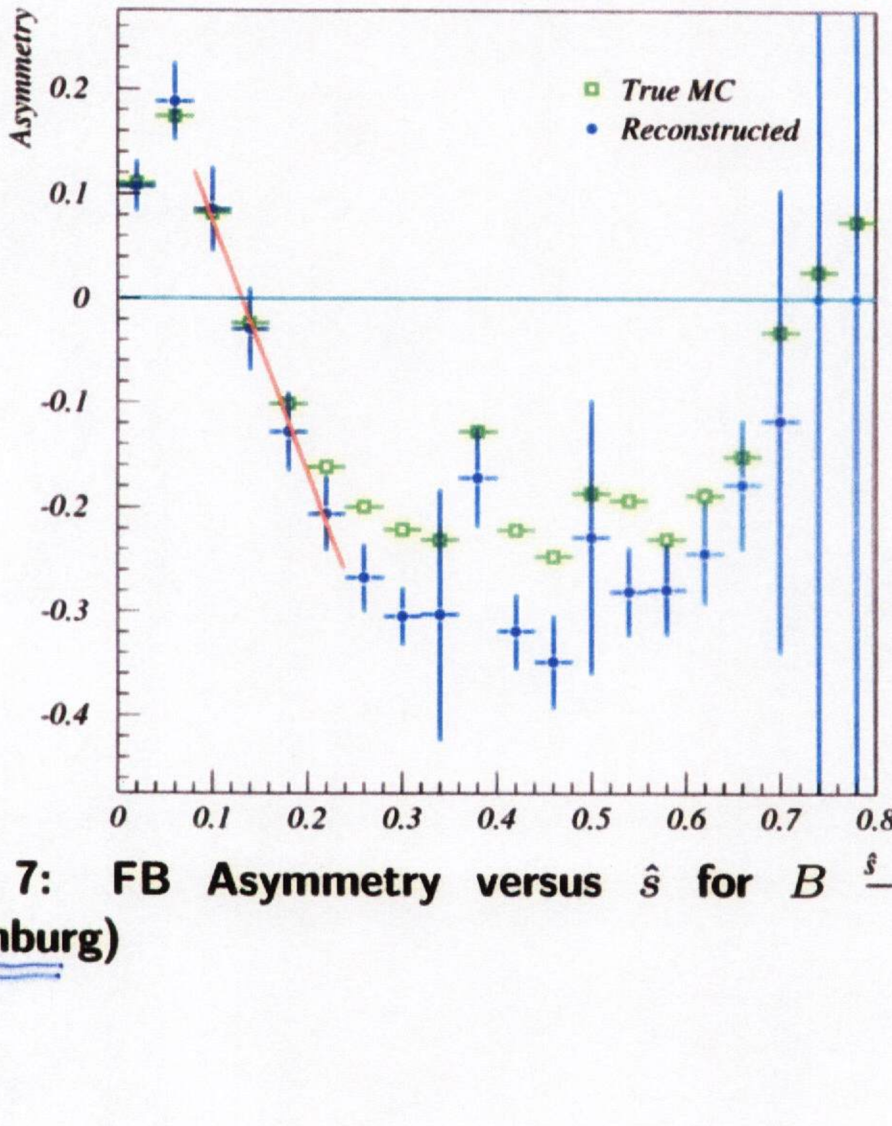

Figure 7: FB Asymmetry versus $\hat{s}$ for $B \xrightarrow{\hat{s}} \mu^+\mu^- K^*$ (from Koppenburg)

The Decays $B \to X_d \ell^+ \ell^-$ & $B_s \to X_s \ell^+ \ell^-$

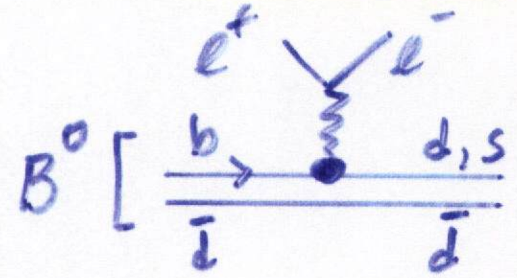
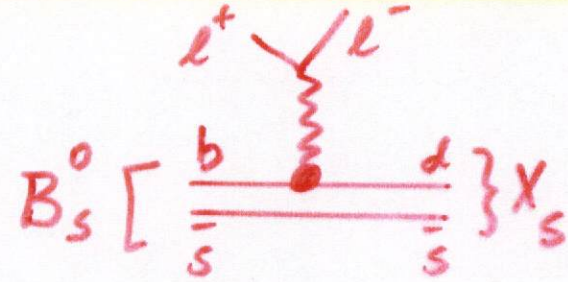

$$\Delta\mathcal{R}_d \equiv \frac{\mathcal{B}(B^0 \to X_d \ell^+ \ell^-)}{\mathcal{B}(B^0 \to X_s \ell^+ \ell^-)}$$

$$= \lambda^2 \frac{(1-\rho)^2 + \eta^2}{1 - \lambda^2(1-2\rho)} \left[1 + \frac{\rho^2 + \eta^2}{(1-\rho)^2 + \eta^2} R_1 + \frac{\rho(1-\rho) - \eta^2}{(1-\rho)^2 + \eta^2} R_2 \right]$$

$$\Delta\mathcal{R}_s \equiv \frac{\mathcal{B}(B_s^0 \to X_s \ell^+ \ell^-)}{\mathcal{B}(B^0 \to X_s \ell^+ \ell^-)}$$

$$= C_{sd} \lambda^2 \frac{(1-\rho)^2 + \eta^2}{1 - \lambda^2(1-2\rho)} \left[1 + \frac{\rho^2 + \eta^2}{(1-\rho)^2 + \eta^2} R_1 + \frac{\rho(1-\rho) - \eta^2}{(1-\rho)^2 + \eta^2} R_2 \right] \ldots$$

- C_{sd} a phase space factor $\simeq 1$; R_1, R_2 calculated in partial NNLO [Hiller,A.A.]; Complete NNLO calculation under way [Greub et al.]
- Measurement of $\Delta\mathcal{R}_d$ or $\Delta\mathcal{R}_s$ will constrain the CKM UT in a very similar fashion as the ratio $\Delta M_d/\Delta M_s$ in the SM; But they measure different quantities in BSM scenarios than $\Delta M_d/\Delta M_s$
- Simulations done for $\Delta\mathcal{R}_d$ at LHCb [Koppenburg]; $\Delta\mathcal{R}_s$ has lesser systematic errors, as final states identical
- Crucial to have good mass resolutions on M_B and M_{B_s}; $M_{B_s} - M_{B_d} = 90.2 \pm 2.45$ MeV $\simeq 7\sigma(M_{B_d})$ at LHCb

Hiller, A.

$$\Delta R \equiv \frac{\mathcal{B}(B \to X_d l^+ l^-)}{\mathcal{B}(B \to X_s l^+ l^-)}$$

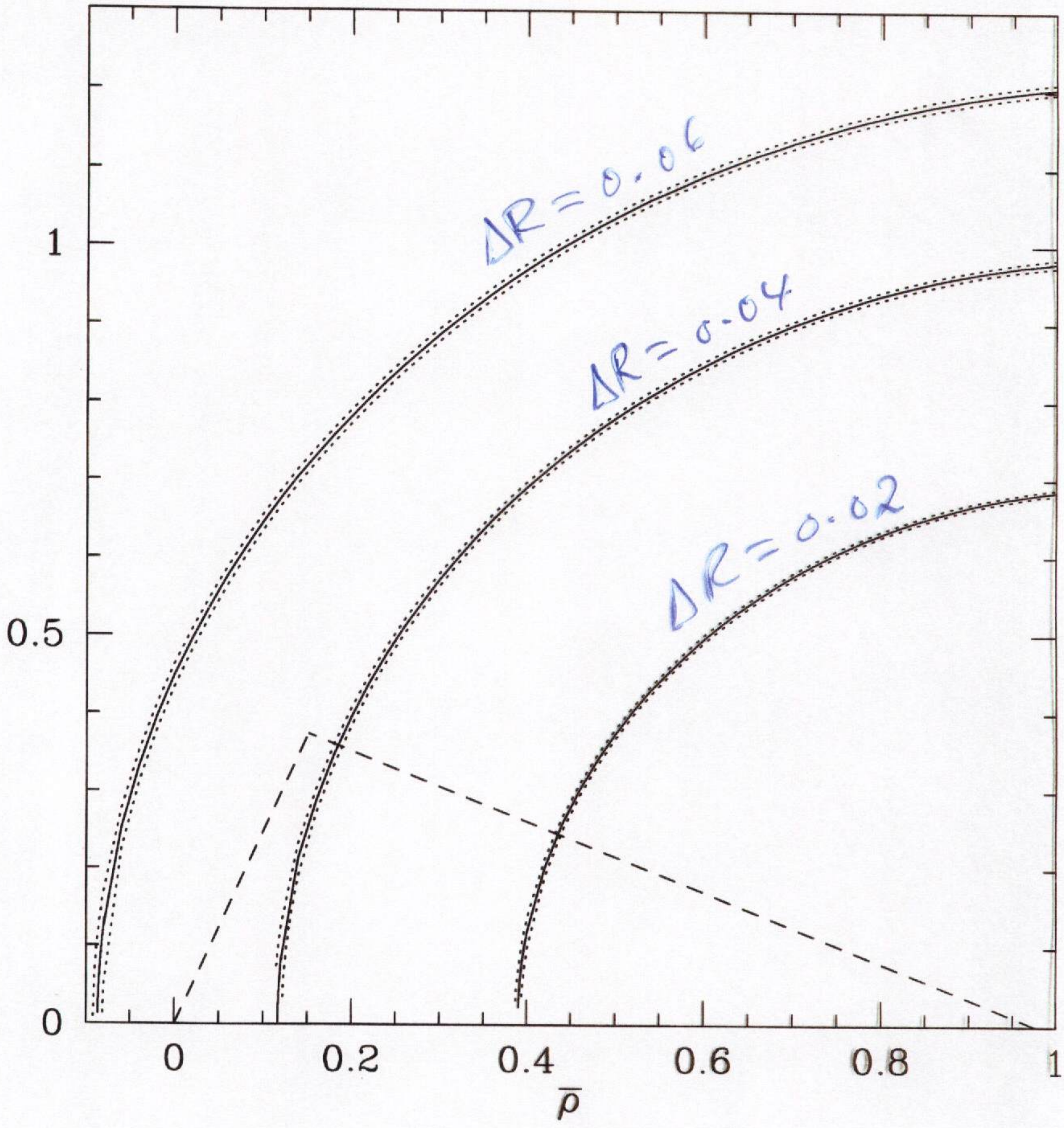

UT - Constraints from ΔR

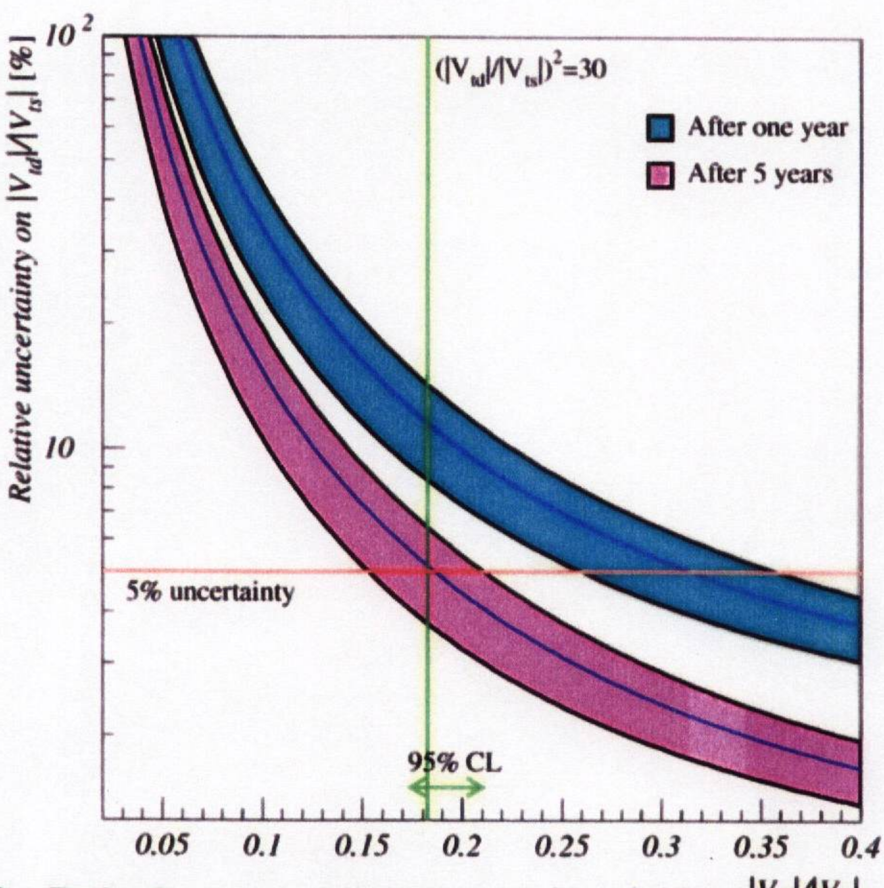

Figure 8: Relative uncertainty on $|V_{td}|/|V_{ts}|$ after one and five years of LHCb (from Koppenburg)

$B \to X_s(X_d)\nu\bar{\nu}$ Decays

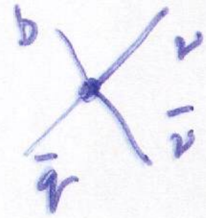

Effective Hamiltonian in SM

$$\mathcal{H}_{eff} = \frac{4G_F}{\sqrt{2}} \frac{\alpha}{2\pi \sin^2\theta_W} \sum_{i=u,c,t} V_{ib}V_{iq}^* \bar{C}_L^i(m_i)(q\gamma_\mu P_L b)(\bar{\nu}_f \gamma^\mu P_L \nu_f)$$

- $C_L^{u}(0) = 0$; $\frac{C_L^c(m_c)}{C_L^t(m_t)} \sim O(10^{-3})$
- $|\frac{V_{cb}V_{cq}^*}{V_{tb}V_{tq}^*}| \sim O(1)$ **(for $q = d, s$)**
  $\Longrightarrow B \to X_s(X_d)\nu\bar{\nu}$ **completely dominated by the top quark contribution; NLO corrections calculated** [Buchalla, Buras]
- **Long-distance contribution negligible** [Buchalla, Isidori, Rey]
- **Branching ratios in the SM** [Buras, Buchalla; Buras]

  $\mathcal{B}(B \to X_s\nu\bar{\nu}) = 3.7 \times 10^{-5} \frac{|V_{ts}|^2}{|V_{cb}|^2} [\frac{\bar{m}_t(m_t)}{170\ \mathrm{GeV}}]^{2.30}$
- **Current Experimental Bound:** $\mathcal{B}(B \to X_s\nu\bar{\nu}) < 7.7 \times 10^{-4}$ **(ALEPH)**
- $\frac{\mathcal{B}(B \to X_d\nu\bar{\nu})}{\mathcal{B}(B \to X_s\nu\bar{\nu})} = \frac{|V_{td}|^2}{|V_{ts}|^2}$

  Cleanest direct determination of $\frac{|V_{td}|}{|V_{ts}|}$!
- **Likewise, Exclusive Decays $B \to (K, K^*, \pi, \rho)\bar{\nu}\nu$ theoretically clean**

BABAR: $\mathcal{B}(B^+ \to K^+\nu\bar{\nu}) < 9.4 \times 10^{-5}$ [SM: 3.8×10^{-6}]

- **Decay rates sensitive to new physics (in particular supersymmetry)** [Recent NLO analysis: Bobeth, Buras, Krüger, Urban '01]; **but measurements challenging!**

b → $q\nu\bar{\nu}$ in NLO

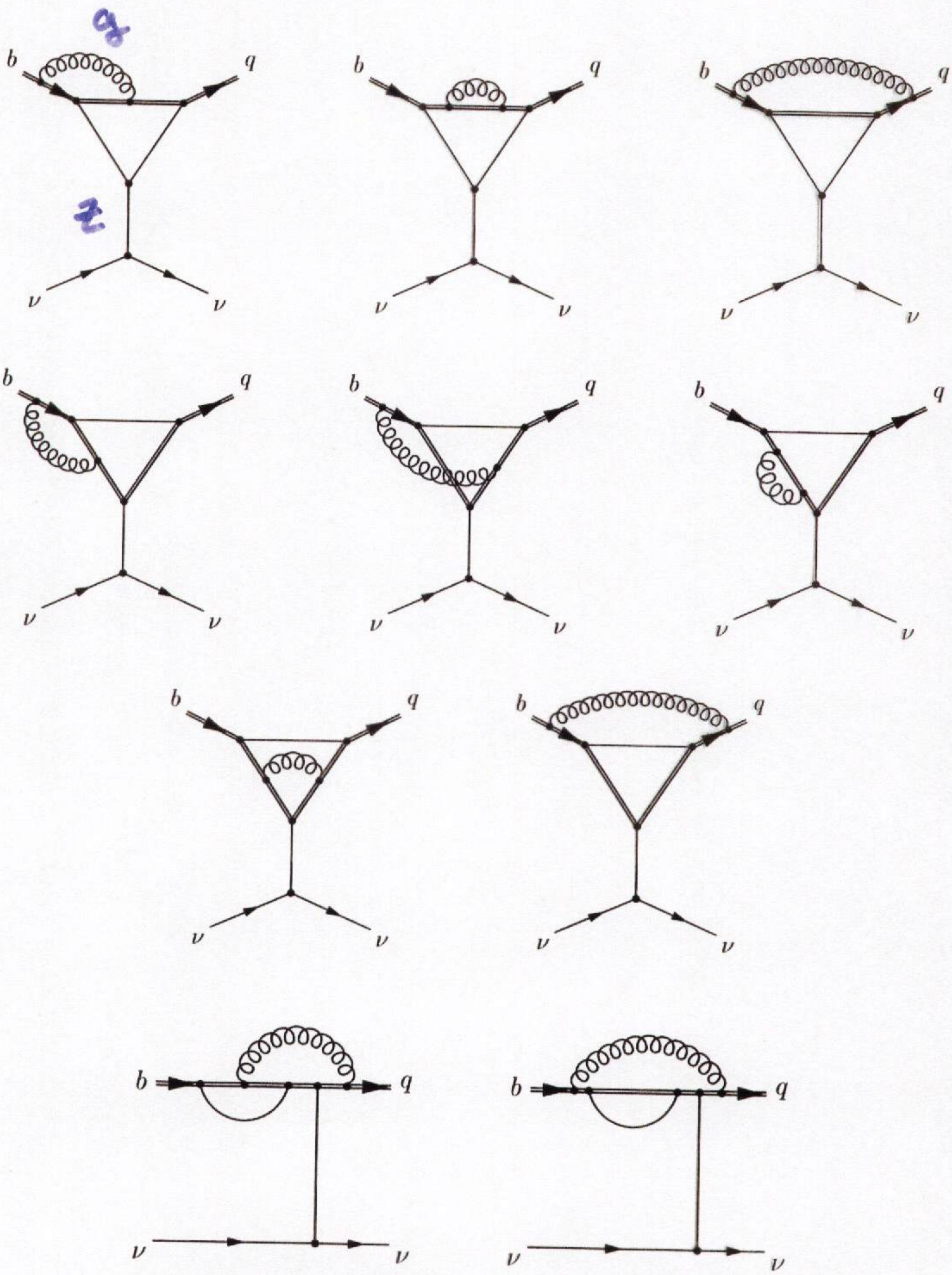

Figure 1: Penguin diagrams contributing to the transition $b \to q\nu\bar{\nu}$ ($q = d, s$) at order α_s. The vertical and curly lines denote Z^0 bosons and gluons, respectively, while the coloured particles (i.e. quarks and their superpartners) are represented by double lines. The diagrams for $b \to ql^+l^-$ may be obtained by replacing $\nu \to l$ and by taking into account neutral Higgs and would-be-Goldstone bosons, in addition to the Z^0 boson. The corresponding symmetric diagrams are not shown here.

$B \to K\nu\bar{\nu}$ results (BaBar)

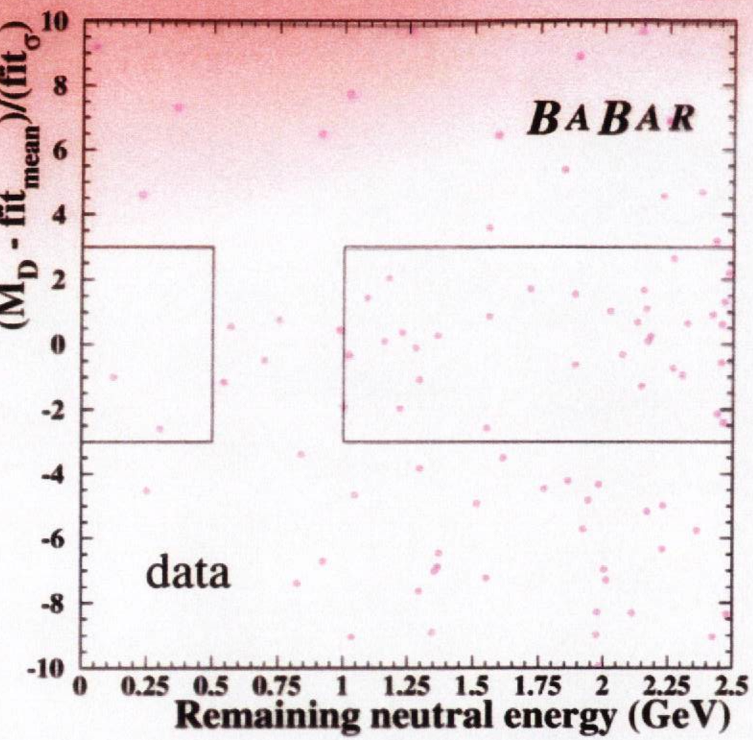

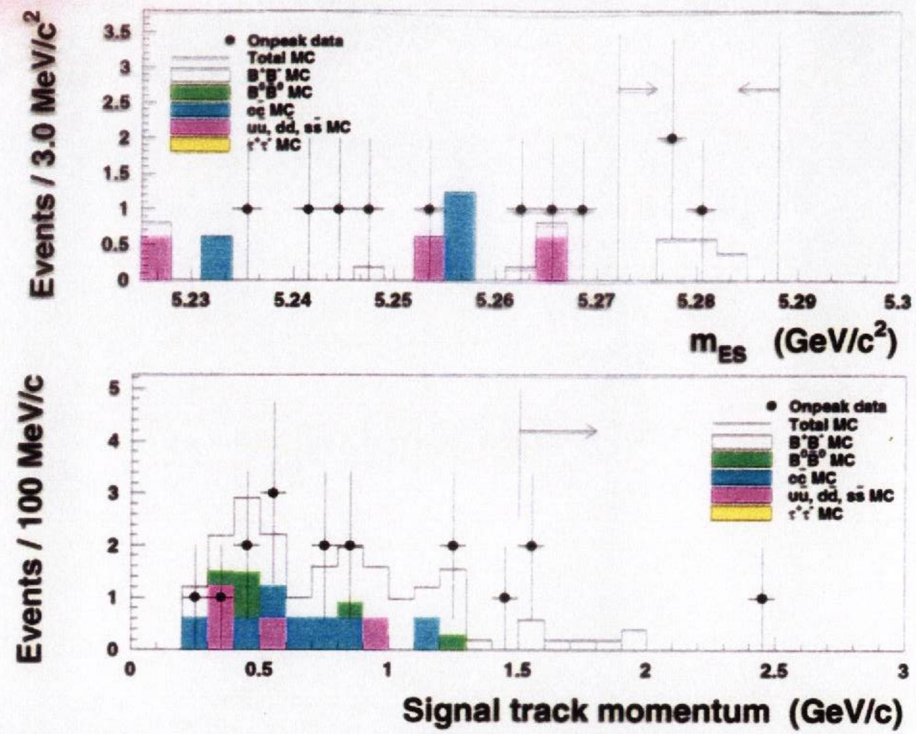

Semileptonic tag (D^0 and ℓ^-)

51 fb^{-1}, 2 candidates

2.2 background expected

$\mathcal{B}(B \to K\nu\bar{\nu}) < 9.4 \times 10^{-5}$

Hadronic tag ($(D(n(\pi))^-$)

80 fb^{-1}, 3 candidates

2.7 ± 0.8 background expected

$\mathcal{B}(B \to K\nu\bar{\nu}) < 10.5 \times 10^{-5}$

combined: $\mathcal{B}(B \to K\nu\bar{\nu}) < 7.0 \times 10^{-5}$ (90% C.L.)

SM: $\mathcal{B}(B \to K\nu\bar{\nu}) = (3.8^{+1.2}_{-0.6}) \times 10^{-6}$ [Buchalla,Hiller,Isidori 2000]

$B_s(B_d) \to \ell^+\ell^-$ Decays

Effective Hamiltonian in SM

$$\mathcal{H}_{eff} = -\frac{G_F}{\sqrt{2}}\frac{\alpha}{2\pi \sin^2\theta_W} V_{tb}^* V_{tq} Y(x_t)(\bar{b}q)_L(\bar{\ell}\ell)_L$$

- **Dominated by the top quark contribution; NLO corrections calculated** [Buras, Buchalla]
- **SM Estimate** [Buras]**:**

$$\mathcal{B}(B_s \to \mu^+\mu^-) = 3.3\times 10^{-9}[\frac{\tau(B_s)}{1.5\ \mathrm{ps}}][\frac{F_{B_s}}{210\ \mathrm{MeV}}]^2[\frac{V_{ts}}{0.04}]^2[\frac{\bar{m}_t(m_t)}{170\ \mathrm{GeV}}]^{3.12}$$

$$\frac{\mathcal{B}(B_d \to \mu^+\mu^-)}{\mathcal{B}(B_s \to \mu^+\mu^-)} = \frac{\tau(B_d)}{\tau(B_s)}\frac{m_{B_d}}{m_{B_s}}\frac{F^2_{B_d}}{F^2_{B_s}}\frac{V^2_{td}}{V^2_{ts}}$$

$$\Longrightarrow \quad \mathcal{B}(B_d \to \mu^+\mu^-) = O(10^{-10})$$

- **Current Experimental Bounds:**
  $\mathcal{B}(B_s \to \mu^+\mu^-) < 2.0\times 10^{-6}$ **[CDF]** $\longrightarrow$ 1.0×10^{-6}
  $\mathcal{B}(B_d \to \mu^+\mu^-) < 6.1\times 10^{-7}$ **[CLEO]** $\longrightarrow$ 1.6×10^{-7}
  $< 2.1\times 10^{-7}$ [BABAR] [HFAG '03]
- $\mathcal{B}(B_s \to \mu^+\mu^-)$ **measurable at LHC**
- **In BSM, huge enhancement possible; a case in point supersymmetry in large** $\tan\beta$ **region** [Many authors; more recently: Bobeth, Buras, Krüger, Urban]
  G. D'Ambrosio, G.F. Giudice, G. Isidori, A. Strumia

$B \to \ell^+\ell^-$ results (Belle)

- New results based on 78 fb^{-1} (supersedes FPCP'03 Belle results)

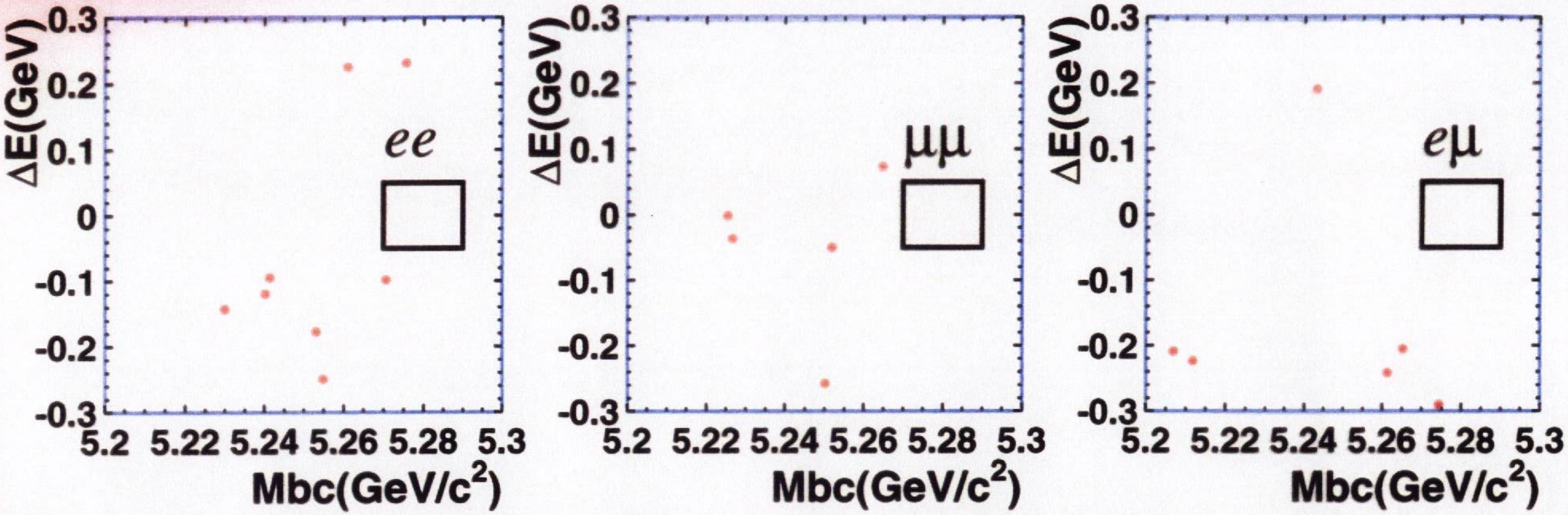

	efficiency	Observed ev.	Expected b.g.	BF (90% C.L.)
$B^0_d \to e^+e^-$	14.3%	0	0.30 ± 0.12	$< 1.9 \times 10^{-7}$
$B^0_d \to \mu^+\mu^-$	16.9%	0	0.19 ± 0.10	$< 1.6 \times 10^{-7}$
$B^0_d \to e^\pm\mu^\mp$	15.8%	0	0.22 ± 0.10	$< 1.7 \times 10^{-7}$

B($B_s \to \mu^+\mu^-$) [Bobeth, Buras, Krüger, Urban]

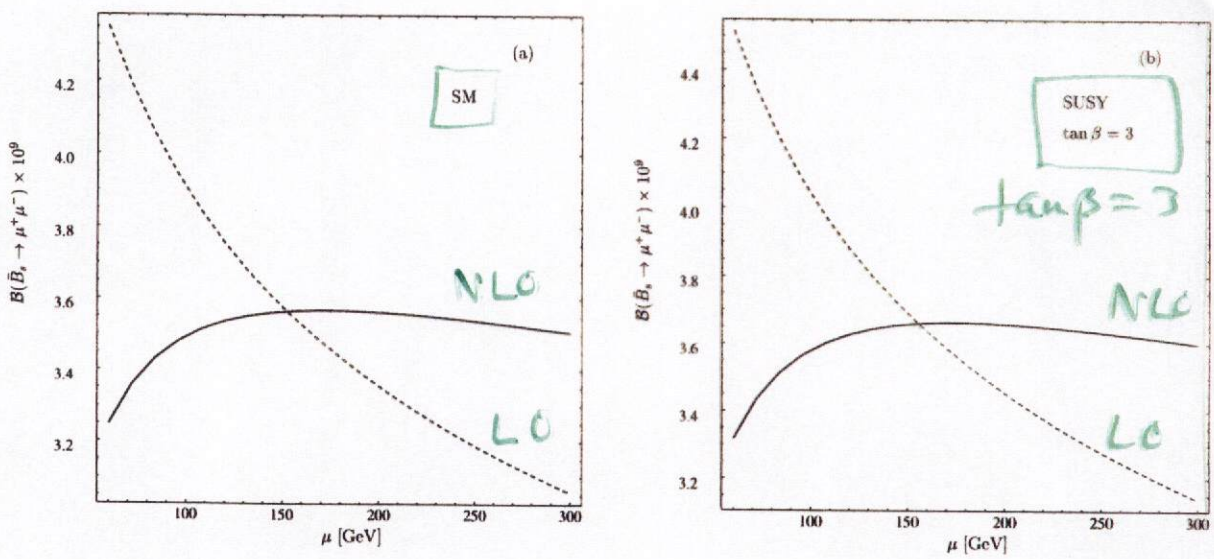

Figure 7: The μ dependence of the $\bar{B}_s \to \mu^+\mu^-$ branching ratio for (a) the SM, and (b) SUSY in the low $\tan\beta$ regime, as defined in Eq. (6.6). The solid and dashed curves denote the predictions with and without QCD corrections, respectively.

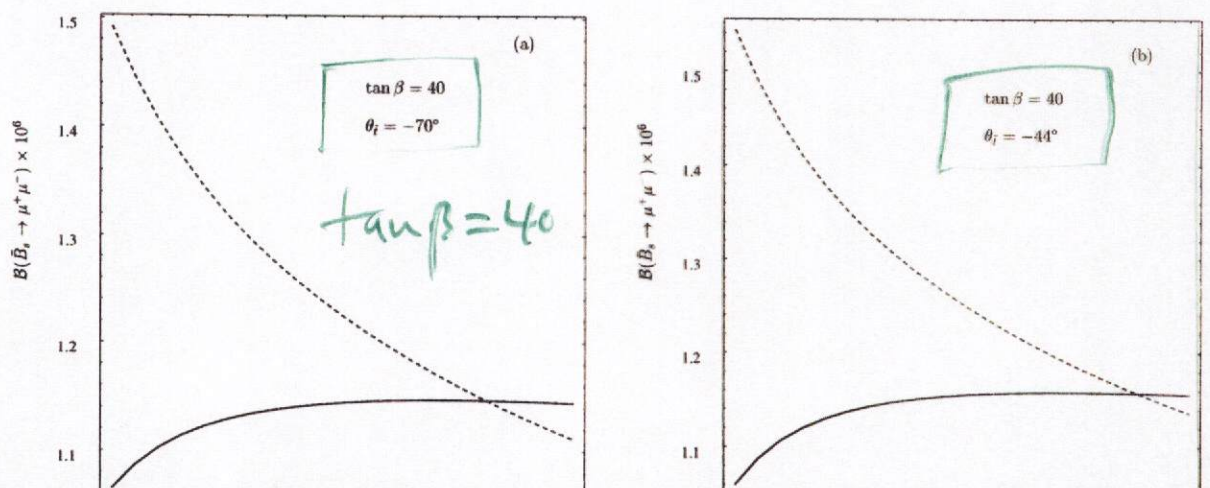

Figure 8: The μ dependence of the $\bar{B}_s \to \mu^+\mu^-$ branching ratio within SUSY at large $\tan\beta$. The solid and dashed curves denote the SUSY prediction with and without QCD corrections, respectively. (a) For the case of a predominantly right-handed light stop quark, using the SUSY input parameters given in Eq. (6.7). (b) For the case of almost maximal mixing in the scalar top quark sector according to the parameter set given in Eq. (6.8). Note the order-of-magnitude enhancement of the branching ratio, compared to the SM and low $\tan\beta$ SUSY predictions in Fig. 7.

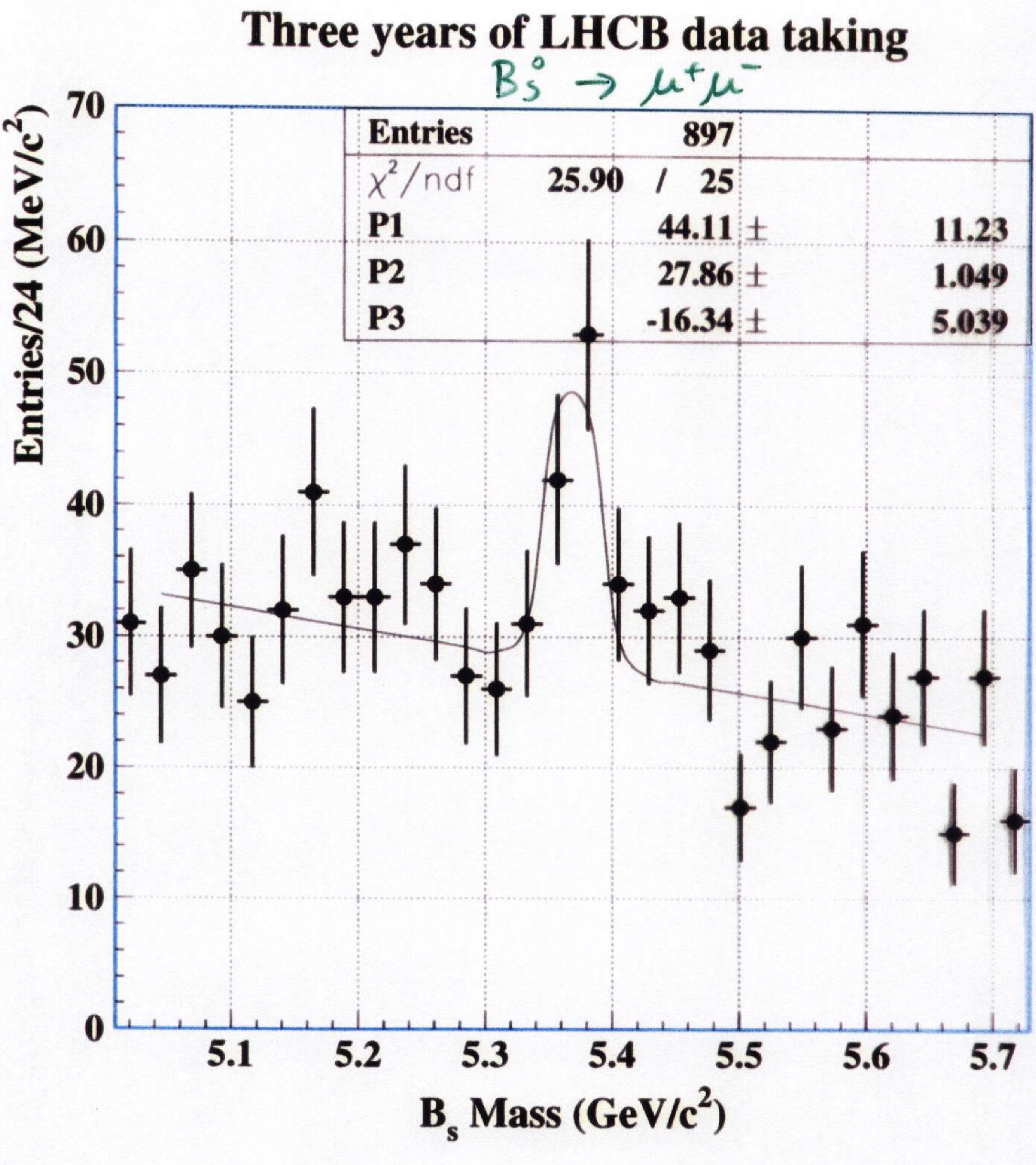

Figure 9: Mass plot of $B_s^0 \rightarrow \mu^+\mu^-$ events after three years of LHCb data taking (from Polycarpo)

Summary of new results

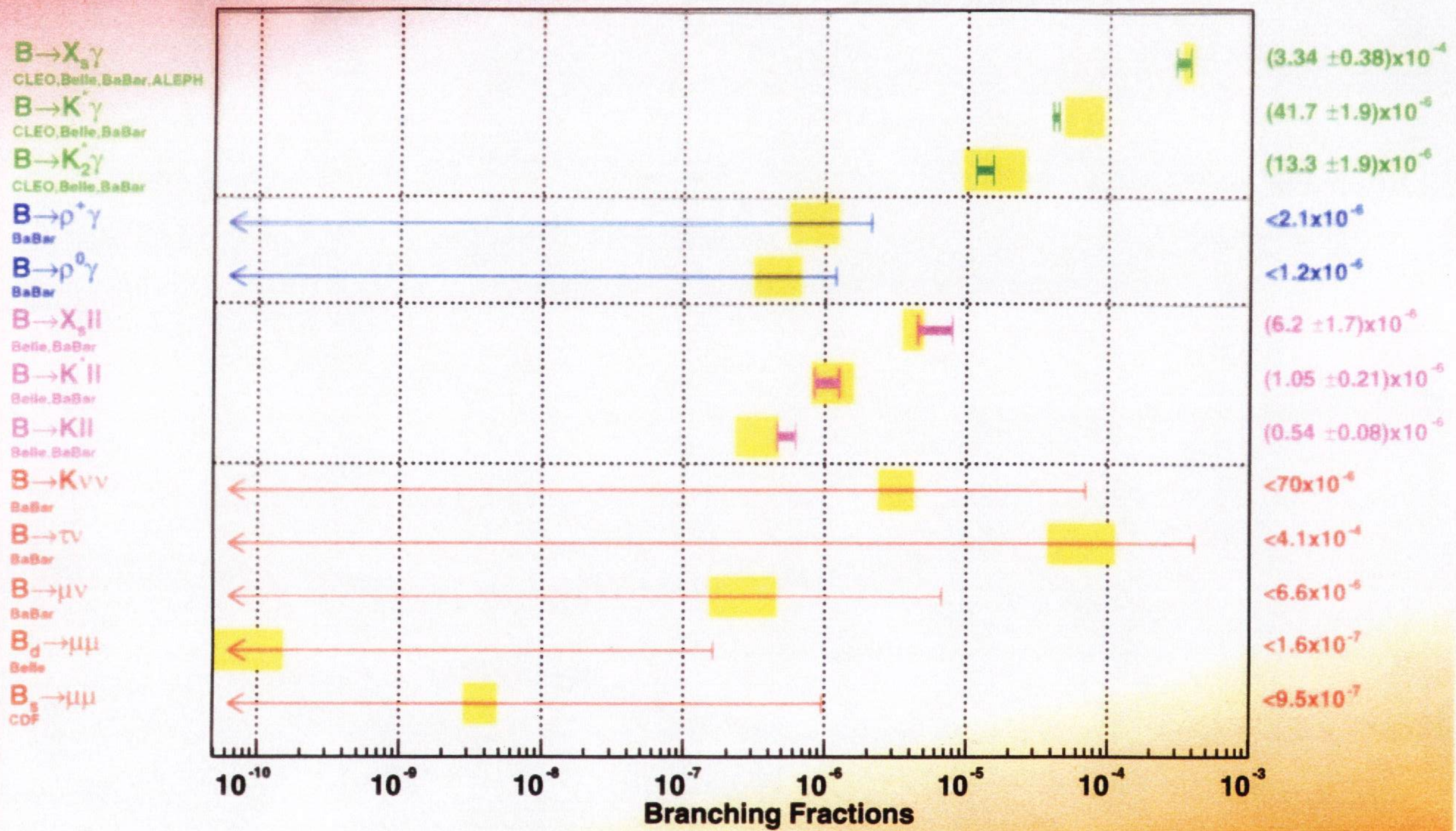

Summary on Rare B Decays

- At a Super-B-Factory, anticipated experimental precision on $\mathcal{B}(B \to X_s\gamma)$ is $\mathcal{O}(1\%)$; Need to improve SM Precision; $B \to X_s\gamma$ will continue to provide valuable constraints on SUSY parameters even in the LHC-era

- SM is in agreement with $\mathcal{B}(B \to K^*\gamma)$ at 30% level; Theory limited at present by the precision on FFs; Isospin violation $\Delta_{0-}(K^*\gamma)$ and $\mathcal{A}_{\rm CP}(K^*\gamma)$ may reveal Physics beyond the SM

- $B \to \rho\gamma$ and $B \to \omega\gamma$ will be measured at the current B-factories; First measurements of $B \to X_d\gamma$ will be available from Super-B Factories; $b \to d\gamma$ transitions provide valuable tests of the SM, such as the measurement of the angle α, and in searching for possible effects from SUSY through partial rates, CP- and isospin-asymmetries

- Inclusive Decays $B \to X_s\ell^+\ell^-$ under theoretical control; Precise measurements of the Dilepton Spectra in $B \to (X_s, K, K^*)\ell^+\ell^-$ and Forward-Backward Asymmetry in $B \to (X_s, K^*)\ell^+\ell^-$ crucial tests of SM
- The Decay $B_s \to \mu^+\mu^-$ is a test case for Large-$\tan\beta$ Supersymmetry
- Likely Scenario: Supersymmetry will be dicovered at LHC (squarks, gluinos,...); some information will be at hand on couplings, perhaps also on the nature of the LSP. However, study of the SUSY-Flavour sector requires precision experiments in the B-sector, which will be carried out at the LHC-(B) and Super-B Factories

- Very Exciting Times are Ahead of us!